SOME PROBLEMS IN HYDRODYNAMICS AND AERODYNAMICS TREATED THEORETICALLY AND EXPERIMENTALLY.

SUDHIR RANJAN SENGUPTA., B.Sc.

Introduction.

The thesis consists of four papers, viz: (Paper.I.) Flow through a Grid ~~consisting~~ comprises of Cylindrical Bars of Circular Cross section, (Paper.II) Losses at Sudden Enlargement and Contraction in Two Dimensions, (Paper.III) Flow in a SemiCircular Bend of a Channel of Rectangular Section and (Paper.IV. as an additional paper) Air Torque on a Cylinder Rotating in an Air Stream. The last mentioned paper had been done in conjunction with Dr.A.Thom. All these have been done in the Aeronautics Laboratory of the James Watt Engineering Laboratories of the Glasgow University, under the direction of Professor J.D.Cormack Director of Laboratories. The writer wishes to thank Professor Cormack for advice and guidance and for the facilities given to him. ~~Thew~~ The writer is also indebted to Dr.Thom for help and advice throughout.

The writer wishes to express his indebtedness to the Department of Scientific and Industrial Research for the grant of a Maintenance Allowance (1931-33) which enabled him to fully carry out the work embodied in papers 2,3, and 4 and the major portion of the work of paper I . Paper I, has been completed with financial assistance from the Carnegie Trust, and the writer is also indebted to the Carnegie Trust for granting him a Research Scholarship (1933-34).

Index.

Index (Contd)

Note:--- For the Diagrams of the Papers I, II and III, please see Book II of the thesis.

FLOW THROUGH A GRID COMPOSED OF CYLINDRICAL BARS OF CIRCULAR CROSS-SECTION.

List of Symbols used in Paper I

d	= diameter of the Cylinder.
l	= length of the Cylinder.
ρ, μ, ν	= density, viscosity, and kinematic viscosity of fluid.
U	= undisturbed velocity.
R	= Reynold's Number.
2c	= distance between centres of cylinders, or distance between channel walls.
2	= distance between two point vortic~~i~~es in the same row.
2	= distance between two rows of point vortices.
U_1	= velocity of vortic~~i~~es in channel
ΔU	increment in the mean velocity of flow past cylinder due to channel wall interference
K_D''	= Total drag coefficient for a cylinder of the Grid
K_P	= Pressure " ,, ,, ,,
K_V'	= Viscous " ,, ,, ,,
K_D'	= Increment in total drag coefficient due to interferenc
K_D	= Total drag coefficient for single cylinder.
K_D	= ,, ,, ,, ,, ,, ,, placed in channel with a parabolic s velocity distribution.

(FLOW THROUGH A GRID CONSISTING OF CYLINDRICAL BARS OF CIRCULAR CROSS-SECTION)

SUMMARY.

(I) Part I deals with flow of perfect fluid past the Grid for $d/2c = 1/2$ and for $d/2c=2/3$ - , ie, with the solution of $\nabla^2\psi = 0$.

Electrical analogy is applied to check the approximate solution obtained. Increase of electrical resistance of a plate of uniform thickness due to the presence of circular hole is obtained from theory and experiment.

A method of estimating the increased velocity of flow past cylinder due to interference is given based on perfect fluid motion.

(2) Part II deals with the arithmetical solution of viscous flow past the Grid $d/2c = 1/2$ at Reynold's Number 20

There does not seem to exist a stationary eddy pair at this Reynolds Number. This is confirmed by photographing the wake of the cylinder of the Grid. (cf, case of Single Cylinder)

Values of K_P, K_V and K''_D are obtained from the above solution and are found to be higher than those for a single cylinder in infinite field at the same Reynolds Number.

(3) Part III deals with the solution of Boundary Layer equation for the Grid $d/2c = 1/2$ at $R = 851$

The viscous drag coefficient K_v for a cylinder of the Grid d/2c = I/2 is found to be $\cancel{\xi}$, 2,4I / $\sqrt{R}$

(4) Part IV gives an approximate estimate of the front generator pressure of a Cylinder of the Grid d/2c = I/2 based on Boundary Layer Theory. This is found to be greater than ~~the~~ that for a single cylinder. Approximate estimate of this for the Grid d/2c = I/2 is also given from the experimental pressure curves.

(5) Part VI deals with experiments.

Pressure drag is calculated from pressure measurements round a Cylinder of the Grid d/2c = I/2 .

Total drags of a Cylinder of the Grid d/2c = I/2 and d/2c = 3/IO are obtained from direct force measurements.

Total drag of Cylinder od the Grid d/2c = I/2 is also obtained by measuring the loss in total head.

The drag coefficients are found to be greater than those for a single cylinder in infinite field.

The viscous drag coefficients K_v for a cylinder of the Grid d/2c = I/2 as obtained from the experiments is found to be 3/ $\sqrt{R}$ as compared to 2/ $\sqrt{R}$ for single cylinder.

(6) Part VII deals with the Karman Vortex Street behind the Grid. It is found to be unstable.

(7) In Part VIII, the writer uses Rosenhead and Scwabe's particulars of Karman street behind a cylinder between channel walls to estimate the total drag coefficients for a clinder of Grid for different values of d/2c.

(8) In Part IX an approximate expression for the total drag the ratio of the total drag coefficients of a cylinder of the Grid or for a cylinder between parallel walls to that of a cylinder in infinite field is given.

(9) In Part X an alternative expression for the increased velocity of flow past cylinder due to interference, is given based on the increased drag coefficients.

(10) In Part XI an approximate estimate of the Increased drag of a cylinder between channel walls, when the velocity distribution is parabolic is given.

PART I.

FLOW OF PERFECT FLUID.

1. The equation of motion of perfect fluid can be written as

$$\nabla^2\psi \equiv \frac{\partial^2\psi}{\partial x^2} + \frac{\partial^2\psi}{\partial y^2} \equiv \frac{\partial v}{\partial x} - \frac{\partial u}{\partial y} = 0 \qquad \text{..........} \; (1)$$

where ψ is the stream function and u and v are the x and y components of velocity, respectively. This equation admits of the introduction of the conjugate velocity potential function ϕ, given by

$$\nabla^2\phi = 0 \qquad \text{..........} \; (2)$$

such that ϕ and ψ are conjugate.

2. A mathematical solution of the problems involving the equations (1) and (2) is theoretically possible by the use of conjugate functions such as

$$\phi + i\psi = f(x+iy) + F(x-iy)$$

Such a transformation satisfying the boundary conditions presents considerable difficulties. The necessary boundary conditions to be satisfied in this problem are

(i) ψ = constant, say equal to zero, when y = o, and when $x^2 + y^2 = \frac{d^2}{4}$

(ii) ψ = constant say KC when $y = \pm c$

(iii) $\frac{\partial\psi}{\partial y}$ = -U when $x = \pm \infty$

and

(iv) $\frac{\partial\psi}{\partial y}$ = o , when $x = \frac{d}{2}$, $y = o$;

where d = diameter of the cylinder.

2c = distance between centres of cylinders.

-U = Undisturbed velocity.

(See Fig. 1).

3. Professor Lamb has given a solution (Ref. 1), which satisfies these conditions when the diameter d is small compared to the distance 2c between the centres of neighbouring cylinders. This can be written as

$$\psi = -U\left\{ y - \frac{\pi d^2}{8c} \frac{\sin\frac{\pi y}{c}}{\cosh\frac{\pi x}{c} - \cos\frac{\pi y}{c}} \right\} \qquad \text{........... (3)}$$

4. When d is not small compared to 2c, an approximate solution can be obtained by the use of Schwarzian transformation, as has been done by Mr Page (Ref. 2). An alternative transformation has been suggested by Professor T. M. MacRobert; this also does not give any better result.

5. Although several methods have been suggested to get round curved boundaries by Schwarzian transformation (Refs. 3, 4) none of these seems to yield perfect circles in the Z-plane.

6. The corresponding potential problem has however been recently solved by Mr. Kiichirô Ochiai (Ref. 5) by expressing the potential at a point in the form of an integral equation and solved by choosing a set of orthogonal functions. The evaluation of these entails certain amount of approximation. The use of such a method for the present purposes presents formidable mathematical difficulties.

7. A mathematical solution giving an oval closely approximating a circle can be got by the following transformation, which appears to be due to Müller (Ref. 6) and has been recently used by Richter (Ref. 7) in solving the analogous permeability problem

$$\phi + i\psi = -ZU + D \coth \frac{\pi Z}{2c} \qquad \text{...........} \quad (4)$$

where $Z = x + iy$

and $D =$ constant.

Separation of the real and the imaginary parts gives

$$\phi = U\left(x + D \frac{\cosh \frac{\pi x}{c} + \cos \frac{\pi y}{c}}{\sinh^2 \frac{\pi x}{c} + \sin^2 \frac{\pi y}{c}} \sinh^2 \frac{\pi x}{c}\right) \qquad \text{....} \quad (5)$$

and

$$\psi = U\left(y - D \frac{\cosh\frac{\pi x}{c} + \cos\frac{\pi y}{c}}{\sinh^2\frac{\pi x}{c} + \sin^2\frac{\pi y}{c}} \sin^2\frac{\pi y}{c}\right) \quad \ldots (6)$$

The constant D is determined from the condition that $\frac{\partial\psi}{\partial y} = 0$ when $x = \frac{d}{2}$, $y = 0$.

$$\frac{\partial\psi}{\partial y} = U\left[1 - D\frac{\pi}{c}\left\{\frac{\cosh\frac{\pi x}{c}\cos\frac{\pi y}{c} + \cos\frac{2\pi y}{c}}{\sinh^2\frac{\pi x}{c} + \sin^2\frac{\pi y}{c}} - \frac{\left(\cosh\frac{\pi x}{c}\sin\frac{\pi y}{c} + \frac{1}{2}\sin\frac{2\pi y}{c}\right)\sin\frac{2\pi y}{c}}{\left(\sinh^2\frac{\pi x}{c} + \sin^2\frac{\pi y}{c}\right)^2}\right\}\right] \quad \ldots (7)$$

Equating equation (7) to zero, we get

$$D = \frac{2c}{\pi}\sinh^2\frac{\pi d}{4c} \quad \ldots\ldots\ (8)$$

Thus we finally get

$$\psi = -U\left\{y - \frac{2c}{\pi}\sinh^2\frac{\pi d}{4c}\frac{\cosh\frac{\pi x}{c} + \cos\frac{\pi y}{c}}{\sinh^2\frac{\pi x}{c} + \sin^2\frac{\pi y}{c}}\sin^2\frac{\pi y}{c}\right\} \quad \ldots (9)$$

From equation (9) it is seen that $\psi = 0$ when $y = 0$ and $\psi = 0$ when

$$\frac{\pi y}{2c}\frac{1}{\sinh^2\frac{\pi d}{4c}} = \cot\frac{\pi y}{2c} \quad \ldots\ldots\ (10)$$

From equation (10) it may be shown that d^1, the minor axis of the oval as obtained from equation (9) is almost equal to the major axis d of the same oval. Table (I) gives the approximate values of d^1 for different ratios of $\frac{d}{2c}$.

8. As seen from the above discussions all these available mathematical solutions ~~treatments~~ give approximately circular boundaries.

It was thought necessary, with a view to ~~in the interests of~~ the latter part of the paper (Part II), to solve the problem for accurate ~~by maintaining the strict boundary conditions~~ boundaries with sufficient accuracy by the use of successive approximations.

There are several methods of approximate treatment available, such as those due to Bairstow and Berry (Ref. 8), Thom (Ref. 9) and to Winny (Ref. 10).

The method ~~one~~ employed is ~~that~~ due to Thom (Ref. 9) ~~and The~~ It ~~method~~ consists in dividing the field into squares of sides 2n (Fig. 2) and expressing the value of ψ at the centre of a square in terms of the ψ values at the corners of the square by expanding ψ in a Taylor series up to the third order terms. The centre value ψ_0 is then given by

$$\psi_0 = \psi_M = \frac{\psi_A + \psi_B + \psi_C + \psi_D}{4} \qquad \text{....... (11)}$$

where ψ_A, ψ_B, ψ_C, ψ_D are the assumed values of ψ at the four corners. Such centre values ψ_0 as obtained by using equation (11) are used as corner values to find the ψ values at the original corners. The process is repeated till the field is settled. values converge to a limit ?

9. Although it has not been possible to give a formal proof of convergence of this method of solution, it has been found to be convergent in numerical computation provided the squares are reasonably small in size.

A11 An approximate proof convergence, however, has been given by Thom and Orr (Ref. 11).

A simple approximate proof of convergence is given below. For the sake of simplicity it is assumed that the part of the field taken is divided into four squares (Fig. 2). The sides BC, CE and GH, HK, coincide with the boundary of the field, hence the values of ψ are definitely known. Then

$$\psi_{O_1} = \psi_{M_1} + K_1 = \frac{\psi_A + \psi_B + \psi_C + \psi_D}{4} + \frac{\epsilon_A + \epsilon_D}{4} \qquad \ldots (12)$$

where ψ_{M_1} is the value of ψ at the centre of square from equation (11), ψ_{O_1} is the correct value of ψ at O, and K_1 is the error and equal to $\psi_{O_1} - \psi_{M_1}$, ϵ_A and ϵ_D are errors in ψ at the corners A and D due to neglecting terms of order higher than the third in equation (11). Hence,

$$K_1 = \frac{\epsilon_A + \epsilon_D}{4} = K_4$$

$$K_2 = \frac{\epsilon_D + \epsilon_F}{4} = K_3$$

(explicit definition of K_2?)

The correction to (Error in using) (11) (giving a closer approximation to find a better value) for ψ_D is then

$$e = \frac{\epsilon_A + \epsilon_F}{8} + \frac{\epsilon_D}{4} \qquad \ldots\ldots\ldots\ldots (13)$$

Using this modified value of ψ_D to evaluate ψ_{M1} the error involved is say K_1', and then

$$K_1' = \frac{\epsilon_A}{4} + \frac{\epsilon_A + 2\epsilon_D + \epsilon_F}{32} = K_4'$$

$$K_2' = \frac{\epsilon_F}{4} + \frac{\epsilon_A + 2\epsilon_D + \epsilon_F}{32} = K_3'$$

Hence, when using the new centre value ψ_M to evaluate ψ_D the error involved e_1 is

$$e_1 = \frac{5}{32}(\epsilon_A + \epsilon_F) + \frac{\epsilon_D}{16} \qquad \text{.........} \ (14)$$

From equation (13) and (14) it is easily seen that $e_1 < e$, and the process is convergent if

$$\frac{5}{32}(\epsilon_A + \epsilon_F) + \frac{\epsilon_D}{16} < \frac{\epsilon_A + \epsilon_F}{8} + \frac{\epsilon_D}{4}$$

if $$\frac{1}{32}(\epsilon_A + \epsilon_F) < \frac{3}{16}\epsilon_D$$

From a consideration of the terms neglected in equation (11) the quantities ϵ_A, ϵ_F, ϵ_D can be assumed to be of the same order as ϵ say. Hence $e_1 < e$ if $\frac{1}{16}\epsilon < \frac{3}{16}\epsilon$

Hence the process is convergent, since the error term is convergent.

A

10. A straightforward method of solving any problem is to assign suitable assumed values to corners of squares into which the

field is divided and use equation (11) repeatedly over and over again till the ψ values become stationary at each corner. A comparatively simple method is to work with differences of ψ values at each corner, when the arithmetic can be done mentally, since only small quantities are involved in the calculation. The method of speeding up as suggested by Thom and Orr (Ref. 11) can also be profitably employed.

11. An alternative method of treatment suggests itself in the present case. For a single cylinder in infinite field the stream function values η are known throughout the field from the equation

$$\eta = -U \frac{y(x^2 + y^2 - 1)}{x^2 + y^2} \qquad \text{........... (15)}$$

The values of ψ on line y = c in this field can be obtained by substituting c in equation (15). But in the present case on line y = c, i.e., LL^1 in Fig. (1) the values stream functions ψ is constant, say B. Hence the correction e to ψ values as obtained from equation (15) on line y = c on the boundaries is obtained from

$$e = B + U \frac{y(x^2 + c^2 - 1)}{x^2 + c^2} \qquad \text{........... (16)}$$

The value of stream function on y = o, and on the circle $x^2 + y^2 = \frac{d^2}{4}$ is zero in equation (15) as well as in the present field. Hence the correction $\underline{e}$ is zero on the circle and on $y = o$.

The field is now divided into squares and corrections $\underline{e}$ are assumed for the corners of the squares. Equation (11) is then used repeatedly till the correction field is settled; using correction terms $\underline{e}$ instead of ψ values in equation (11).

The correction field for $\frac{d}{2c} = \frac{1}{2}$ is shown in Fig. (3).

The ψ values at each corner of the squares are then obtained by adding the corrections obtained above. The field is then solved for ψ values using equation (11). The skeleton solution is shown in Fig. (4).

The net advantage of this method is that we are dealing with small quantities in the correction field and that we have a reasonably accurate set of values of ψ while using equation (11) in the main field.

The stream lines as obtained from the above solution are shown in Fig. (5).

12. As mentioned by Thom (Ref. 12) considerable difficulty arises at a curved boundary because it is impossible to arrange matters so that the boundary passes through the corners of all the squares it cuts. Accordingly some method of interpolation has to be used to obtain the ψ values for successive approxi-

mations on the corners of those boundary squares whose outer corners fail to fall exactly on the boundary. A method of overcoming this difficulty in the case of viscous fluid has been given by Thom (Ref. 12). If squares obtained by the network of streamlines and equipotential lines, obtained by solving $\nabla^2\psi = o$, $\nabla^2\phi = o$ for given boundaries, are used instead of squares formed by the x - y network, the above difficulty is overcome; since the corners of the squares then ~~land~~ lie on the boundary.

This suggests the use of a network such that the inner boundary (circle, and line y = o) is transformed into a line, and the outer boundary y = c, also into a line. But this is the required solution. If however the transformation for single cylinder in the infinite field, i.e., say $W = \xi + i\eta = Z + \frac{1}{Z}$ is used, the inner boundary is transformed into a straight line and the outer boundary y = c, is transformed into a curve given by the following equation in the W-field

$$\frac{\xi}{\eta} = \frac{x}{c}\;\frac{x^2+c^2+1}{x^2+c^2-1} \qquad \text{.............. (17)}$$

The curvature of this line (See Fig. 6 for $\frac{d}{2c} = \frac{1}{2}$ and Fig. 7 for $\frac{d}{2c} = \frac{2}{3}$) is small and consequently interpolation is much easier. The line y = c is accurately drawn in W-field, and the field is divided into squares and ψ values are assigned to the corners of the squares. Equation (11) is then used along with successive interpolation of the ψ values at the corners of the squares near the outer boundary y = c.

This method has been proved to be very quick and the outline solutions for $\frac{d}{2c} = \frac{1}{2}$ and $\frac{d}{2c} = \frac{2}{3}$ are given in Figures (6) and (7) respectively.

Figures (8) and (9) show the streamlines in the w-field as obtained from the above solutions.

Figures (5) and (10) show the ψ lines at equal intervals in the x - y field for $\frac{d}{2c} = \frac{1}{2}$ and $\frac{d}{2c} = \frac{2}{3}$ respectively.

The above solutions (Figs. 6, 7, 8, 9) ~~can be regarded as that for~~ are exact for channels of the shape as shown in the figures.

13. An alternative method of obtaining ψ, ϕ has been suggested by Thom (Ref. 13). This consists in solving for x, y in the ψ, ϕ network. The above methods however suit the peculiarities of the problem and proved more suitable.

14. The velocity q at any point on the x - y field is obtained from the w-field from the following equation

$$
\begin{aligned}
q^2 &= u^2 + v^2 \\
&= \left(\frac{\partial\psi}{\partial\eta}\right)^2 (u_1^2 + v_1^2) \\
&= \left(\frac{\partial\psi}{\partial\eta}\right)^2 q_1^2
\end{aligned}
$$

i.e. $q = q_1 \frac{\partial\psi}{\partial\eta}$ .... (18)

Where q_1 is the velocity in the w-field for single cylinder due to the transformation $W = Z + \frac{1}{Z}$.

15. The pressures and the velocities on the surface at various angles θ from the leading ~~front~~ generator of the cylinder are given in Table II for $\frac{d}{2c} = \frac{1}{2}$, and $\frac{d}{2c} = \frac{2}{3}$.

These are shown plotted in Figures (11) and (12) respectively, along with those for single cylinder in infinite fluid.

16. There is an exact ~~mathematical~~ analogy between flow of electric current along a sheet of uniform thickness (is analogous to that of) and irrolational motion in hydrodynamics. If $t = \rho\sigma$ then $V = \phi$, $W = \psi$ where V and W are electric potential and current functions; and

$$\left.\begin{aligned} \frac{\partial\psi}{\partial x} &= \rho v, & \frac{\partial\psi}{\partial y} &= -\rho u \\ \frac{\partial\phi}{\partial x} &= -u & \frac{\partial\phi}{\partial y} &= -v \\ \frac{\partial\psi}{\partial y} &= tf = \frac{t}{\sigma}\frac{\partial V}{\partial x} \end{aligned}\right\} \qquad \text{.............} \quad (19)$$

This analogy provides us with a method of checking the above arithmetical solution.

If two points A and B on the line $y = c$ are taken, then the drop of potential between A and B can be calculated by integrating $\frac{\partial\psi}{\partial y}$ along AB, since

$$\int_A^B \frac{\partial\psi}{\partial y}\,dx = \rho\int_A^B \frac{\partial\phi}{\partial x}\,dx = \frac{t}{\sigma}\int_A^B \frac{\partial V}{\partial x}\,dx. \qquad \text{.............} \quad (20)$$

From the solution obtained by the approximate methods $\frac{\partial\psi}{\partial y}$

is evaluated by careful numerical differentiation and the potential drop is evaluated by careful mechanical integration. For $\frac{d}{2c} = \frac{1}{2}$ the increase in resistance is found to be the same as that produced by an additional length of n x 2c i.e. (n times the width of plate) added to the plate, where n = 0.4807.

17. As no data were available for comparison it was decided to carry out a set of resistance measurements. [Note] Resistance of a strip of eureka (length 3.327", breadth 1.012" and thickness 0.015") was measured by Wolff Potentiometer, first with no holes and then with holes of different diameters. The experimental results are shown in Table III along with ~~that~~ those obtained theoretically.

The values of n (0.4791) as obtained experimentally for $\frac{d}{2c} = \frac{1}{2}$, is in close agreement with 0.4807 as obtained by the approximate method.

The values of n are shown plotted against $\frac{d}{2c}$ in Figure (12)a.

18. From the above analogy it is seen that the lines of equal velocity potential are obtained by tracing the electric equipotential lines. Fig. (13) shows the equipotential lines as traced by the wire bridge method, for $\frac{d}{2c} = \cancel{\frac{1}{2}}$ 0.497, magnified four times by means of a pantagraph.

Note:- The writer is indebted to Mr. A. J. Small, B.Sc., for helping him with the resistance measurements.

19. The presence of equidistant parallel channel walls increases the mean velocity past the cylinder by constricting the tubes of flow (preventing the expansion or bulge of the streamlines.) A provisional method of correcting for this increase has been given by Thom (Ref. 9) for $\frac{d}{2c}$ less than $\frac{1}{5}$.

An approximate method of correcting for the increase in velocity based on perfect fluid motion is obtainable from the above solutions. It is seen from Fig. (1) that the rows of cylinders may be considered as images on the parallel planes LL^1 and MM^1, thus producing parallel channel walls, and the cylinder may be regarded as being placed at the centre of two parallel walls distance 2c apart. For a single cylinder in a infinite perfect fluid the velocity on the surface of the cylinder is given by

$$q = 2U \sin\theta \qquad \text{..........} \quad (21)$$

where U is the undisturbed velocity and is maximum and equal to 2U when $\theta = \frac{\pi}{2}$ measured from the leading front generator of the cylinder.

The average velocity on the surface is therefore

$$q' = \frac{2}{\pi}\left\{2U\int_0^{\frac{\pi}{2}} \sin\theta \, d\theta\right\} = \frac{2}{\pi}\left(2U\right) \qquad \text{..........} \quad (22)$$

i.e. $\frac{2}{\pi}$ times the maximum circumferential velocity.

For a row~~s~~ of cylinders ~~i.e.~~ or its equivalent a single for cylinder ~~in~~ between parallel channel walls the circumferential velocity q can be written as

$$q = U m \sin\theta \qquad \text{..........} \quad (23)$$

where ~~M~~ m is not a constant, but a function of θ and m is equal to

m_1 when $\theta = \frac{\pi}{2}$.

Hence the average velocity on the surface is

$$\frac{2}{\pi}\int_0^{\frac{\pi}{2}} q.d\theta \equiv \frac{2}{\pi}U\int_0^{\frac{\pi}{2}} m \sin\theta \, d\theta \qquad \text{......... (24)}$$

Hence the increment in the average velocity ΔU due to the presence of channel wall is given by

$$\Delta U = \frac{2}{\pi}\left\{\int_0^{\frac{\pi}{2}} q \, d\theta - 2U\right\} \qquad \text{......... (25)}$$

$$\frac{\Delta U}{U} = \frac{2}{\pi}\left\{\int_0^{\frac{\pi}{2}} m \sin\theta \, d\theta - 2\right\} \qquad \text{......... (26)}$$

A first approximation to (25) is obtained by assuming $m = \text{constant} = \frac{m_1 + m_o}{2}$ and then

$$\frac{\Delta U}{U} = \frac{2}{\pi}\left(\frac{m_1 + m_o}{2} - 2\right) \qquad \text{......... (27)}$$

A good approximation to the correction is obtained if we assume that the average velocity can be taken as the arithmetic mean of the velocity on the ~~zone~~ front leading generator and of the maximum velocity (i.e. at 90^o); then the increment in velocity ΔU is given by

$$\Delta U = \frac{1}{2} q_m - U \qquad \text{......... (28)}$$

where q_m is the maximum velocity on the surface of the cylinder at 90^o in the case of the cylinder between parallel walls.

The increase in velocity ΔU as calculated from (26) and (28) is shown in Table IV for various ratios of $\frac{d}{2c}$.

Figure (14) shows $\frac{\Delta U}{U}$ plotted on $\frac{d}{2c}$. The ~~law~~ relation between $\Delta U/U$ connecting and $\frac{d}{2c}$ can be expressed as

$$\frac{\Delta U}{U} = \frac{0{\cdot}04}{\left(1 - \frac{d}{2c}\right)^2} + \frac{0{\cdot}18}{\left(1 - \frac{d}{2c}\right)} - 0{\cdot}22 \qquad \text{............ (29)}$$

PART II.

STUDY OF VISCOUS FLOW AT LOW REYNOLD'S NUMBER.

1. The equations of steady viscous flow in two dimensions reduce to

$$\nu \nabla^2 \zeta = u \frac{\partial \zeta}{\partial x} + v \frac{\partial \zeta}{\partial y}$$

and $$\nabla^2 \psi = 2\zeta \qquad \ldots\ldots\ldots (30)$$

where $u = -\dfrac{\partial \psi}{\partial y}$, $v = \dfrac{\partial \psi}{\partial x}$

A rigid mathematical solution of the equation (30) has been ~~possible~~ found only in a few cases.

2. A simplified form of the hydrodynamical equations which holds for infinitely low Reynold's number has been given by Oseen (Ref. 14). A second approximation to Oseen equations has been given by Filon (Ref. 15), but this also holds for very low Reynold's number.

3. Solutions of flow past a single cylinder in infinite fluid for Reynold's number of the order of 0·2 have been given by Lamb (Ref. 16) and by Bairstow, Cave and Lang (Ref. 17). Thom has given solution of equation (30) by the use of an arithmetical method, for this problem for Reynold's Number 10 (Ref. 9) and Reynold's Number 20 (Ref. 12). Thom's solutions are of consider-

able interest, especially the one at R = 20, where he obtains a "stationary eddy pair," as is experimentally found to exist. The range of this method of solution is probably up to R = 35 for the single cylinder, above which the motion behind the cylinder is no longer stable.

4. There does not appear to be any theoretical solution in existence for the viscous flow past a row of cylinders. There is, however, in existence a solution for the allied problem i.e. of flow past a cylinder between two parallel walls (for $\frac{d}{2c} = \frac{1}{5}$) by Bairstow, Cave and Lang (Ref. 18). This solution is probably valid up to Reynold's number of the order of 0·2

5. The differences between the present problem and that dealt by Bairstow and Lang are that in the present case the vorticity values on the line of symmetry (LL^1 in Fig. (1)) is zero and that the velocity is uniform in the undisturbed parts of the field; whereas in the latter, there is definite vorticity ~~on~~ at the channel walls and the velocity distribution is parabolic in the undisturbed portion of the channel. The flow past a row of cylinders may therefore be regarded as flow past a single cylinder between parallel walls with the above ~~limitations~~ differences!! Consequently Bairstow's method of solution could have been used, but as mentioned above such a solution would only be valid up to R ≑ 0·2

6. It was, therefore, decided to use Thom's approximate method, which is quite easy to handle for $\nabla^4\psi = 0$, ~~i.e.~~ for Reynold's number of the above order. The problem with $\frac{d}{2c} = \frac{1}{2}$, has however been solved for R = 20 which is of more interest, because a comparison with the existing R = 20 solution for single cylinder could then be made, and because it would be less troublesome to give experimental verification at this comparatively high Reynold's number.

7. Thom's method of solution (Ref. 9) of equation (30) is one of repeated interpolation in a field of assumed values of ζ and ψ. The field is divided into squares of sides 2n and the values of ζ and ψ are assigned at each corner of the squares. These assumed values for corners give ζ_c and ψ_c for the centre of the squares (see Fig. 15), when the following interpolation formulae are used

$$\zeta_c = \zeta_M - \frac{1}{168}\left\{(a-c)(B-D) + (b-d)(C-A)\right\} \qquad \text{....... (31)}$$

$$\psi_c = \psi_M - n^2\zeta_c \qquad \text{....... (32)}$$

where

$$\psi_M = (A + B + C + D) \div 4 \qquad \text{....... (33)}$$

and

$$\zeta_M = (a + b + c + d) \div 4 \qquad \text{....... (34)}$$

and A, B, C, D are the corner values of ψ and a, b, c, d, are the corresponding values of ζ.

Having used equations (31) to (34) to find the values at the centres of all squares, these centre values are used again in the ~~above~~ same equations to find new values at the original corners.

At solid boundaries the values on the surface are obtained from the approximate expression

$$\zeta_s = (\psi_G - \psi_s) \div n^2 \qquad \text{...........(35)}$$

where ψ_s and ψ_G are values of ψ on the surface and at a point G, distant <u>n</u> from the surface respectively.

8\. Although it has not been possible to give a general formal proof of convergence of the above method, involving the repeated use of equations (31) to (34) in conjunction with equation (35), it has been found to be convergent and to give results closely in agreement with experimental results provided the squares used are not too large (Refs. 9, 12).

9\. Some of the difficulties attending curved boundaries in this method of solution have been mentioned in Part I ~~of this paper~~. In addition to the difficulty of interpolating the values of ψ and ζ at the corners of the squares which do not ~~land~~ lie on the boundary, there is the further difficulty of evaluating the ζ values on the curved surfaces. Thom has shown (Ref. 12) that both these difficulties are overcome if the squares in the W-plane formed by the network of stream lines and equipotential lines obtained by solving $\nabla^2\psi = 0$, $\nabla^2\phi = 0$, for the given boundary conditions are used with similar interpolation formulae (31) to (35). These are

$$\zeta_C = \zeta_M - \frac{1}{16\gamma}\left\{(a-c)(B-D) + (b-d)(C-A)\right\} \qquad \text{......} (36)$$

$$\psi_C = \psi_M - \frac{n^2 \zeta_C}{q_1^2} \qquad \text{..........} (37)$$

and $$\zeta_S = (\psi_G - \psi_S)\frac{q_2^2}{m^2} \qquad \text{..........} (38)$$

Where the subscript M indicates the mean of the corner values of ζ and ψ of the squares of sides 2n in the W-plane and q_1 is the velocity of transformation and in equation (38) ψ_G is the value of ψ_S at point G, distance m from the boundary in the W-plane and q_2 is the mean of the velocities of transformation at the surface and at the point G.

10. The work outlined in Part I was undertaken partly with a view to obtain this network. But as mentioned there, although ψ values obtained by methods in Part I are reasonably accurate, the ϕ values could not be regarded as good enough for use in this part of the paper. When the transformation due to Müller (which could be taken to represent the irrotational problem) ~~was~~ became available, the work outlined here ~~has~~ had been almost completed, by recourse to an alternative method.

11. As in Part I if the transformation $W = Z + \frac{1}{Z}$ is used, the circle and the line $y = o$ transforms into a straight line and $y = c$ transforms into a curved line in the W-field. This transformation has been used in solving the case when $\frac{d}{2c} = \frac{1}{2}$. The advantage of the use of this field instead of the Z-field has been mentioned partly in Part I. There is also the further advantage due to the fact that on this curved line $(y = c)$ in the W-field the vorticity is zero and hence we get over the difficulty of evaluation of ζ on the curved outer boundary. Thus part of the advantages of the use of $\nabla^2\psi = o$ field satisfying the boundary conditions have been obtained by this method. There was also the further advantage that q_1^2 values as involved in equations (36) to (38) were directly obtainable from Dr. Thom's detailed solution.

12. The solution is given for $R = 20 = \frac{Ud}{\nu}$ using the following values

d = diameter of the cylinder = 2.

U = Undisturbed Velocity = 1.

$\nu = 0.1$

$\frac{d}{2c} = \frac{1}{2}$

Sheets were prepared for the W-plane so that the ordinary squared paper could be used. Values of ζ and ψ were assigned to the corners of the squares, keeping Thom's solution at R = 20 for a single cylinder as guide. Formulae (36) to (38) were applied hundreds of times until the field has reasonably settled. Various speeding up methods have been employed, some of which have been communicated by Dr. Thom (Ref. 13).

13. Skeleton solutions of the front and of the rear portion of the cylinder are shown in Figures (16) and (17) respectively. It was found necessary to use very small squares near the front generator - possibly because this is a singular point in the W-field. Figure (18) shows the skeleton solution for the greater part of the field. The various necessary precautions have been discussed thoroughly elsewhere (Refs. 9, 12), and as such these are not mentioned here.

It is to be noticed from Figure (17) that there is no stationary eddy at the rear part of the cylinder, as exists in the case of a single cylinder at the same Reynold's number (Ref. 12).

The stream lines as obtained in the above solution are shown in the W-field in Figure (19). By means of $\xi - \eta$ network and cross plotting the actual stream lines are obtained and these are shown in Fig. (20). ~~Fig. (21) is the corresponding figure for single cylinder (Ref. 12)~~.

14. To determine the pressure at any point A in the field it is necessary to integrate along a line from some point B (where the

pressure is already known) to the point A. In the present example B is taken at such a distance from the cylinder that the flow there is undisturbed by the cylinders. Necessary expressions for use in the W-field are given by (Refs. 9, 12)

$$p_A + \tfrac{1}{2}\rho q_A^2 = p_B + \tfrac{1}{2}\rho q_B^2 - 2\rho\nu \int_A^B \frac{\partial \zeta}{\partial \xi}\, d\eta + 2\rho \int_A^B \zeta \frac{\partial \psi}{\partial \eta}\, d\eta$$

.... (39)

for a line parallel to η axis

and

$$p_A + \tfrac{1}{2}\rho q_A^2 = p_B + \tfrac{1}{2}\rho q_B^2 + 2\rho\nu \int_A^B \frac{\partial \zeta}{\partial \eta}\, d\xi - 2\rho \int_A^B \zeta \frac{\partial \psi}{\partial \xi}\, d\xi$$

.... (40)

for a line parallel to ξ axis

where p_A , p_B are the pressures and q_A , q_B are the velocities at points A and B respectively.

15. The pressure on the front generator was obtained by integrating along $\eta = 0$ and also by integrating along $\eta = \frac{1}{4}$, $\xi = 2$ in the W-field. The mean of these two is 1.386 $(\frac{1}{2}\rho U^2)$ (See Part IV) as compared to 1.33 $(\frac{1}{2}\rho U^2)$ for single cylinder at the same Reynold's number (Ref. 12).

16. Pressures at other points on the cylinder surface were obtained by integrating along $\eta = \frac{1}{4}$, and ξ = constant lines in the W-field. The results are shown in Table V.

These values are shown plotted in dotted lines in Fig. (26) along with the experimental pressure curves.

The pressure drag is easily obtained by integrating p cos θ round the cylinder. Expressed as a coefficient, $K_p = 1.751$ for the present case ($\frac{d}{2c} = \frac{1}{2}$) as compared to 0.624 for single cylinder (Ref. 12).

17. It has been shown by Thom (Ref. 9) that the intensity of the tangential force at a point on the surface is $2\mu\zeta_0$ where ζ_0 is the vorticity value at the point. Hence the viscous drag can be obtained by integrating ($2\mu\zeta_0$ sin θ) round the cylinder. The values, obtained from the solution are given in Table V. The viscous drag coefficient K_v is found to be 0.835 as compared to 0.433 for single cylinder (Ref. 12). Thus the total drag coefficient K''_D at R = 20 for the cylinder in grid is 2.586 as compared to 1.057 for single cylinder in infinite field (Ref. 12). These coefficients K''_D, K_p and K_v are shown plotted in Fig. (30) along with the experimental results.

18. As seen from figures (17), (19) and (20) there does not seem to exist any stationary eddy behind the cylinder at R = 20 whereas

such eddy pair is found to exist theoretically (Ref. 12) and experimentally for a single cylinder in infinite field at R = 20. It was therefore decided to photograph the stationary eddy pairs. These are shown in Plate (I). ~~Plate (II) shows the eddies as obtained by Thom (Ref. 12) for comparison~~. The first sign of a very minute eddy seems to appear at $R \doteq 25$ in the present case, whereas Thom obtains a fair-sized eddy at R = 12 for single cylinder. Hence the absence of eddy pair as indicated in the solution is justified in the light of the photographs in Plate (I). It would therefore appear that one effect of channel wall constriction is to delay the formation of these stationary eddies.

PART III.

STUDY AT HIGH REYNOLD'S NUMBER OF THE BOUNDARY LAYER PROBLEM.

1. The viscous forces on a body can be predicted at all Reynold's number by the theoretical solution of the Prandtl Boundary Layer Equations at any one Reynold's number if the pressure distribution curve round the body is known at that Reynold's number.

2. The Prandtl Boundary Layer equations can be written as follows (Ref. 19)

$$q \frac{\partial q}{\partial s} + \omega \frac{\partial q}{\partial n} = - \frac{1}{\rho} \frac{\partial p}{\partial s} + \nu \frac{\partial^2 q}{\partial n^2} \qquad \text{....... (41)}$$

$$0 = \frac{1}{\rho} \frac{\partial p}{\partial n} \qquad \text{....... (42)}$$

and

$$\frac{\partial q}{\partial s} + \frac{\partial \omega}{\partial n} = 0 \qquad \text{....... (43)}$$

where n and s are measured normal and tangential to the surface, the components of velocity being W and q.

From (42) it is seen that the pressure gradient along the normal to the surface at any point inside the boundary layer is taken as zero. Hence the pressure measured on the surface is taken as the pressure throughout the entire thickness of the boundary layer.

3. There are in existence several methods of solving these equations (for instance Refs. 20, 21). Some of these methods are general in treatment. The case of a single cylinder has been solved by Thom (Ref. 22) and by Green (Ref. 23).

The method adopted here is that due to Thom. on account of its simplicity and speed Although this method is partly mathematical ~~theoretical~~ and partly experimental ~~the~~ Thom's computated results ~~obtained by Thom has been found to be~~ are in good agreement with his own experimental results ~~experiments of Thom~~ (Ref. 22) and with the more ~~recently with those~~ results of Linke (Ref. 24).

Apart from the simplicity and speed of ~~(obtainable in)~~ this method of solution, Thom's approximation seems to be quite justified in the light of Linke's experiments. already stated above

4. The method consists in determining $\frac{\partial q}{\partial n}$ from the pressure curves in theoretical formulae from $\theta = 0$ to $\theta = 60^{\circ}$ (so long as $\frac{\partial^2 p}{\partial \theta^2}$ is positive) and experimentally determining $\frac{\partial q}{\partial n}$ from $\theta = 60^{\circ}$ to $\theta = 90^{\circ}$ to evaluate the viscous forces. The viscous forces in the rear half of the cylinder are ~~is~~ neglected. The method is justified by experiments.

The intensity of surface friction at any point on the front portion of a cylinder can be estimated from the following equations

$$\mu \frac{\partial q}{\partial n} = \rho \, \frac{\nu^{\frac{1}{2}} U^{1\frac{1}{2}}}{r^{\frac{1}{2}}} \, \frac{\sqrt{h\,(1-p_1)}}{F_2'(x)} \quad \text{when } n \to 0 \qquad \ldots\ldots\ (44)$$

where

r = radius of cylinder.

$$p_1 = (p - p_0) \div \tfrac{1}{2} \rho U^2 \qquad \ldots\ldots\ (45)$$

$$h = -\frac{1}{2\sqrt{1-p_1}} \frac{dp_1}{d\theta} \qquad \ldots\ldots\ (46)$$

$$F_2'(x) = 1 \div \sqrt{\tfrac{2}{3}\left(x^3 - 3x + 2 + M + N\right)} \qquad \ldots\ldots\ (47)$$

$$F_2(x) = \int F_2'(x)\, dx. \qquad \ldots\ldots\ (48)$$

$$N = -\frac{3}{2} \frac{\sqrt{1-p_1}}{h^2} \frac{dh}{d\theta} \int_{x=x}^{x=1} f_1(x)\, dx \qquad \ldots\ldots\ (49)$$

$$f_1(x) = x \frac{F_1(x)}{F_1'(x)} \qquad \ldots\ldots\ (50)$$

$$M = 3 \int_{x=x}^{x=1} f_2(x)\, dx \qquad \ldots\ldots\ (51)$$

$$f_2(x) = \frac{1}{F_1'(x)} \int x\, F_1'(x)\, dx. \qquad \ldots\ldots\ (52)$$

$$F_1(x) = \sqrt{2} \log \frac{\sqrt{1-x}\,(\sqrt{3} - \sqrt{2})}{\sqrt{3} - \sqrt{x+2}} \qquad \ldots\ldots\ (53)$$

$$F_1'(x) = 1 \div \sqrt{\tfrac{2}{3}\left(x^3 - 3x + 2\right)} \qquad \ldots\ldots\ (54)$$

$$q = ux. \qquad \ldots\ldots\ (55)$$

$$n = \sqrt{\frac{\nu r}{Uh}} \quad F_2(x) \qquad \text{......... (56)}$$

$$u = U\left(\sqrt{1 - p_1}\right) \qquad \text{......... (57)}$$

These formulae have been used in solving the present case $\left(\frac{d}{2c} = \frac{1}{2} \right)$ for R = 851. The detailed solution is given in Table VI and Table VII for $\theta = 0$ to $\theta = 60^{\circ}$.

5. The ~~sizes~~ dimensions of the channel (5" width) and the cylinder ($\frac{1}{2}$" dia.) used do not permit of experimentally determining $\frac{\partial q}{\partial n}$ for $\theta = 60^{\circ}$ to $\theta = 90^{\circ}$, as had been done by Thom (Ref. 22).

6. From the following consideration a method of obtaining $\left(\frac{\partial q}{\partial n} \right)$ for any value of θ at Reynold's number R from a knowledge of $\left(\frac{\partial q}{\partial n} \right)_1$ at Reynold's number R_1, both satisfying the same boundary conditions, is apparent.

Equation (44) can be written as

$$\mu \frac{\partial q}{\partial n} = \rho \frac{\nu^{\frac{1}{2}} U^{1\frac{1}{2}}}{r^{\frac{1}{2}}} \sqrt{f\left(p_1 , \frac{\partial p_1}{\partial \theta} , \frac{\partial^2 p_1}{\partial \theta^2} \right)} \qquad \text{....... (58)}$$

This can be written as

$$\mu \frac{\partial q}{\partial n} = \rho \frac{\nu^{\frac{1}{2}} U^{1\frac{1}{2}}}{r^{\frac{1}{2}}} \quad C \qquad \text{....... (59)}$$

where C is a constant.

The equation (59) is legitimate if $\sqrt{f\left(p_1, \frac{\partial p_1}{\partial \theta}, \frac{\partial^2 p_1}{\partial \theta^2}\right)}$ may be regarded as constant C. This assumption is not very far from the truth, as can be seen from the pressure curves at different Reynold's number.

With this assumption, for Reynold's number R_1

$$\left(\frac{\partial q}{\partial n}\right)_1 = \frac{e_1}{\mu_1} \frac{\nu_1^{\frac{1}{2}} U_1^{1\frac{1}{2}}}{r_1^{\frac{1}{2}}} C$$

and

$$\left(\frac{\partial q}{\partial n}\right) = \frac{e}{\mu} \frac{\nu^{\frac{1}{2}} U^{1\frac{1}{2}}}{r} C$$

for Reynold's number R

where subscript 1 refers to Reynold's number R_1, at which $\left(\frac{\partial q}{\partial n}\right)_1$ is known. Hence

$$\left(\frac{\partial q}{\partial n}\right) = \left(\frac{\nu_1 r_1}{\nu r}\right)^{\frac{1}{2}} \left(\frac{U}{U_1}\right)^{1\frac{1}{2}} \left(\frac{\partial q}{\partial n}\right)_1 \qquad \text{.......} \quad (60)$$

From Part II, the solution at R = 20 (for $\frac{d}{2c} = \frac{1}{2}$) is known and $\left(\frac{\partial q}{\partial n}\right)_1$ can be determined from this field. Hence at R. = 851 can be determined by using equation (60).

This has been done for $\theta = 90^\circ$ whence $\left(\frac{\partial q}{\partial n}\right)_1 = 5.962$ for R = 20 and thus $\left(\frac{\partial q}{\partial n}\right)$ at R = 851 is equal to 155.

The use of (60) to determine $\left(\frac{\partial q}{\partial n}\right)$ at R = 851 for higher values of θ, from the solution at R = 20, may not be justifiable because of the change in the nature of the flow behind the cylinder.

7. The values of $\frac{\partial q}{\partial n}$ for R = 851 are shown plotted in Fig. (22). From this figure it seems that $\frac{\partial q}{\partial n}$ is zero when θ approximately equal to 97^{o}. This suggests that the break away of the boundary layer takes place at $\theta \doteqdot 97^{o}$ as compared to $\theta \doteqdot 82^{o}$ for a single cylinder (Ref. 23).

8. The viscous drag is obtained by integrating $\mu \frac{\partial q}{\partial n} \sin\theta$ round the cylinder and the viscous drag coefficient K_v is found to be 0.0825.

It has been shown by Thom (Ref. 22) that the skin friction drag Kv is proportional to $\sqrt{\nu / U d}$ i.e. inversely proportional to $\sqrt{R}$. Hence Kv can be expressed as

$$K_v = \frac{A}{\sqrt{R}} = \frac{2.41}{\sqrt{R}} \qquad \ldots\ldots\ (61)$$

where A $\doteqdot$ 2.41, compared to A = 2 for single cylinder (Refs. 22, 24).

9. The thickness δ of the boundary layer is defined as the distance from the surface in which the velocity attains 95% of the outside velocity and it is given in the last column in Table VII.

10. The curve given by $Kv = \frac{2.41}{\sqrt{R}}$ is shown in dotted line in Fig. (30) for comparison with experiments. The experiments give

$A \doteqdot 3$ and it is seen that the agreement is not very good. But it is apparent from equation (61) that for flow past grid ($\frac{d}{2c} = \frac{1}{2}$) the skin friction drag is also higher than that for a single cylinder.

PART IV.

FRONT GENERATOR PRESSURE.

1. It has been shown by Thom (Ref. 25) that for a single cylinder the front generator pressure p, at all speeds unaffected by compressibility ~~is given~~ may be expressed by $\left(1+\frac{C}{R}\right)\frac{1}{2}\rho U^2$ Where C, while dependent on Reynold's number R, can be taken as constant and equal to 8 at all usual speeds. At first sight it ~~would appear~~ might seem that the front generator pressure should also be the same for flow past a grid. But from the following considerations it will be evident that this need not be so.

2. ~~From the consideration~~ In the approximation of the Boundary Layer Theory it can be shown (Ref. 25) that

$$\Delta H = \frac{\rho \nu U}{r} \sqrt{a_0} \qquad \text{.........} \quad (62)$$

where

$$a_0 = \frac{1}{2}\frac{d^2p}{d\theta^2}$$

r = radius

$$\Delta H = p - \frac{1}{2}\rho U^2$$

$$\therefore \quad \frac{\Delta H}{\frac{1}{2}\rho U^2} = \frac{4\sqrt{a_0}}{R} = \frac{C}{R} \qquad \text{..........} \quad (63)$$

where

$$C = 4\sqrt{a_0} \qquad \text{..........} \quad (64)$$

From Part I, i.e. solution for $\nabla^2\psi = 0$, for the flow past grid ($\frac{d}{2c} = \frac{1}{2}$) $a_o = 5.67$ and hence $C = 9.52$, as compared to $C = 8$ for single cylinder.

3. For viscous flow the value of a_o is however less than 5.67. These have been calculated by finding $\frac{d^2p}{d\theta^2}$ from the experimental pressure curves and C calculated from equation (64). These are shown in Table VIII along with a value of C for $\frac{d}{2c} = \frac{2}{3}$ (calculated from perfect fluid pressure gradient). Fig. (23) shows C, plotted on $\log_{10} R$ for the grid ($\frac{d}{2c} = \frac{1}{2}$).

4. As seen from Figure (23) the points are widely scattered, and this is not surprising because of uncertainty in finding $\frac{d^2p}{d\theta^2}$ from the pressure curves, (a correction being required which has got to be corrected) for the size of pressure holes (See Part V). Hence the value of C can only be taken as only approximate. It has not been possible to verify these values by direct experiments.

It is may however ~~to~~ be ~~noticed~~ inferred, that the front generator pressure as determined above, is certainly different from and higher than that for a single cylinder.

5. The value of C as obtained from R = 20, solution in Part II is also higher than that for single cylinder.

Hence it seems clear that the front generator pressure for flow past grid is in excess of that for flow past single cylinder.

PART V.

CORRECTION FOR THE SIZE OF THE PRESSURE HOLES.

1. The pressure as experimentally determined through pressure holes on the surface of the cylinder is not the pressure at the centre of the hole but is the pressure at a point slightly away from the centre towards the front generator of the cylinder. The exact amount of this correction has not been determined for flow past this grid ($\frac{d}{2c} = \frac{1}{2}$) but the correction to angle for single cylinder as given by Thom (Ref. 12) has been tentatively accepted to hold for the flow past grid, namely ~~The correction is given by~~

$$\Delta\theta = \frac{1}{2}\frac{h}{d} \qquad \text{.............. (65)}$$

where h = diameter of the hole.

PART VI.

EXPERIMENTS.

1. Drag forces on a body ~~is~~ are due partly to the pressure differences existing round the body and partly to the fluid friction.
Expressed as coefficients

$$K''_D = K_P + K_\vartheta = \frac{\text{Drag}}{\rho d.l.U^2} \quad \text{.........} \quad (66)$$

where

K''_D	=	Total drag coefficient.
K_P	=	Pressure drag coefficient.
K_V	=	Viscous drag coefficient.
d	=	Cylinder diameter.
l	=	length of cylinder.
U	=	Undisturbed velocity.

2. K_P can be determined by integrating the component of the measured pressures round the cylinder and K_V by direct measurement of the velocity gradient on the surface of the cylinder and integrating $\mu \frac{\partial q}{\partial n} \sin\theta$ round the cylinder. Alternative method of obtaining $\frac{\partial q}{\partial n}$ is given by the Boundary Layer Equations (See Part III). Thus K''_D is determined by adding K_P and K_V so obtained.

3. An alternative method of finding K_V is to find K''_D by direct force measurement or otherwise (see later part of this part) and subtract K_P from K''_D.

In Part III K_V has been determined from the approximate solution of the Boundary Layer Equations. This part of the paper deals with the determination of K_P and K''_D from direct measurements and thus obtaining K_V.

4. Experimental Determination of the Pressure Distribution round a Cylinder, when the cylinder is one of a row forming the Grid.

The apparatus used consists of a channel having a working section 5" x 5" and a form of Chattock Gauge (Ref. 25). The channel has been modified and description of the modified channel has been given by the writer elsewhere (Ref. 26).

For low Reynold's number work oil has been used in the channel in place of water. The difficulties encountered in experimenting with oil have been mentioned by Thom (Ref. 12) and as such are not repeated here.

The arrangement for pressure measurements is shown in Fig. (24).

Instead of the pressure box, the pressure in a static tube S, placed upstream has been used taken to act as the reference pressure datum. The cylinders are housed in holes properly spaced, on $\frac{1}{4}$" thick strip of brass resting on the bottom of the channel. The bevelled brass plates A_1, A_2 (5" x 5" x $\frac{1}{4}$") are placed in front and behind this strip of brass, holding the cylinders to ensure smoothness of flow past the grid. The pressure drop Δp between S and O is first determined with no cylinder (plates + strips in place). The cylinders are then placed in situ and pressure measurements round the centre cylinder are carried out. The absolute ? pressures are obtained by applying the correction Δp to the observed pressure drop between S and the point on the cylinder surface.

The velocity is kept constant by comparison with a calibrated inverted U-gauge coupled to up and down-stream ends of the channel.

From the ~~F~~front generator pressure ~~is used to give~~ the channel velocity ~~. To obtain this~~ is computed by the methods outlined in Part IV have been adopted.

The final results are given in Table (IX) and the pressure curves are shown in Figures (26), (27) and (28) for a range of Reynold's number (from 7.9 to 851.)

Figure (29) shows the pressure plotted for constant values of θ, namely, $\theta = 40^\circ$, 80°, 120° and 160° ~~on~~ against $\log_{10} R$. These show the same characteristics ? as exhibited by the corresponding graph for single cylinder (Ref. 12).

5. Total Drag Measurements.

Total drag has been obtained by directly measuring the force on two short cylinders (0·6324 cm dia x 3·8350 cm long) and (1·2598 cm dia x 3·8735 cm long) with a balance. The sketch of the balance used and the arrangement of cylinders will be found in which contains the leading dimensions of the balance.

At low speeds, the velocity has been determined by timing suspended foreign matters in the liquid over a measured distance; and at high speed, the velocity has been obtained by means of Pitot head and Tilting gauge.

6. Drag forces, deducting ~~for~~ the additional drag due to dis~~c~~ked ends of the (none, Oxford Dictionary) cylinders, ~~as~~ obtained by separate experiments, are given in Table (X) along with the total drag coefficients K''_D.

7. An alternative method of determining total drag suggests itself from the condition of the problem. This is by measuring the loss in total head, as in propeller work. From Figure (1) it is easily seen that if the loss in total head is known between sections LM and L^1M^1 without the cylinders and with the cylinders in place then the drag is given by the difference of the two total head losses integrated over section LM and L^1M^1. (This method has been employed and) the drag coefficients obtained by this method are given in Table (XI).

Figure (33) shows the a typical pressure distribution curve~~s~~ along section L^1M^1.

To avoid any error due to bad velocity distribution, the total head losses have also been measured on two other sections adjacent to the centre section.

The total drag coefficients K''_D as given in Table (XI) are not in very good agreement with these in Table (X) obtained by force measurement, except at high Reynold's number. This is not surprising, when it is borne in mind that the pressure difference between points such as L and M ~~is~~ correspond only ~~due~~ equal to a fraction of a Chattock turn.

8. Values of K''_D as obtained by direct measurement are shown plotted against ~~on~~ $\log_{10}$ R in Figure (31). The points plotted are means of many observations.

Figure (30) shows K''_D as obtained by force measurement, as well as that obtained by loss in total head, plotted on $\log_{10}$ R.

9. Figure (30) also shows K_P as obtained from the pressure measurements. From the difference of the mean K''_D curve and the mean K_P curve, the K_V curve is shown plotted in full line, on a base of $\log_{10}$ R in Figure (30). The relation between ~~law connecting~~ K_V and R can be approximately expressed as

$$K_V = \frac{3}{\sqrt{R}} \qquad \text{......... (67)}$$

as compared with ~~to~~ $K_V = \frac{2.41}{\sqrt{R}}$ obtained from the approx. math. boundary layer Theory in Part III. The latter is shown in dotted lines in the same Figure (30). Although the agreement between the laws connect-
relations between

ing K_V and R, as determined by experiment and as deduced from theory is not very close, it is seen that the viscous drag coefficient K_V is different from that for a single cylinder.

10. Figure (32) shows K''_D for a cylinder of grid $\frac{d}{2c} = 0.3$, plotted on $\log_{10}$ R. The total drag and the coefficients K''_D are given in Table (XII).

PART VII.

KÁRMÁN STREET VORTICES.

1. An attempt has been made to photograph the Karman Street vortices, but these have been found to be unstable. Plate (III) shows the photographs obtained. It is interesting to note that the photograph at R ≑ 62.4 shows a wake, and that at R ≑ 66.4 the attached stationary eddies show signs of instability. Hence it is probable that the transition of the flow pattern behind the cylinder in the grid takes place at R ≑ 62. For single cylinder this transition seems to take place at about R = 35 to 40. Hence one effect of the presence of the neighbouring cylinders, and probably that of channel wall constriction, is to delay the formation of the Karman Street vortices. The other photographs in Plate III show that the vortices are unstable and that they show a tendency to spread out laterally, to mix and to become annihilated.

2. The stability of these such vortices between parallel channel walls has been studied mathematically by L. Rosenhead (Refs. 27, 28, 29). The same criterion holds for the present case. His results can be summarised as follows.

Vortices are stable

(i) only when the axes of vortices coincide with the axis of channel - i.e. axis of symmetry through the cylinder in the present case:

(ii) only unsymmetrical double row is stable

(a) when b is vanishingly small.

When and only when $a = 0.281$ b.

(b) as b increases, the stable cases are obtained by increasing a almost proportionally. This continues till we get to the case when $b = 0.815$ c, $a = 0.256\ b = 0.208$ c (only determine case)

(c) for b greater than 0.815 c, a range of values of a is obtained in which the system is stable.

(d) when $b \geq 1.419$ c. the system is stable for all values of a

where a, b, and c are as shown in Fig. (34).

From the above results it would seem that the Karman Street vortices may be stable.

3. Photographs of Karman Street vortices behind a cylinder between channel walls satisfying various ratios of $\frac{d}{2c}$ have ~~however~~ been obtained by Rosenhead and Schwabe (Ref. 30). It is found that $\frac{a}{b}$ remains constant $= 0.32$ for all values of $\frac{d}{2c}$ up to $\frac{1}{3}$ but there appears to be a breakdown between $\frac{d}{2c} = \frac{1}{3}$, to $\frac{d}{2c} = \frac{2}{3}$, when $\frac{a}{b} \doteqdot 0.45$.

Hence it is not surprising that the vortices have been found to be unstable (for $\frac{d}{2c} = \frac{1}{2}$).

4. There is further the fact that in a channel of this type, there is every possibility of three dimensional disturbances, under the influence of which this double row is unstable (Ref. 31).

5. There is also the fact that the velocity past neighbouring cylinder in the channel is not absolutely uniform and that any lack of uniformity in velocity would tend to make the vortices unstable.

PART VIII.

INCREASE IN K_D OF A CYLINDER DUE TO CHANNEL WALL.

1. It has been mentioned in the earlier parts of the paper (Parts I and II) that the flow past the grid of cylinders can also be looked upon as flow past a single cylinder between two parallel channel walls distant c from the centre of the cylinder. This is legitimate when the fluid is regarded as perfect fluid. Hence the Karman Street vortices in the wake of a cylinder of this grid may be regarded as identical for the same cylinder between parallel walls.

This assumption enables us to determine the increase in drag due to channel wall interference from a study of the Karman Street vortices behind a cylinder of the grid or conversely the increase in drag due to the presence of neighbouring cylinders from observation on Karman Street behind a single cylinder between channel walls.

2. Glauert (Ref. 32) has given an approximate method for calculating this increased drag. Let the increased drag coefficient be K''_D and let the drag coefficient for single cylinder in infinite field be K_D (obtained from Karman's Theory or otherwise) then

$$K''_D = K_D + K'_D \qquad \text{........... (68)}$$

where,

$$K'_D = 32\ \frac{a}{d} \cdot \frac{a}{c} \cdot \left(\frac{w}{U}\right)^2 \qquad \text{...... (69)}$$

where K^1_D is the increase in the drag coefficient due to channel wall interference and u is the velocity of vortices in the corresponding Karman Street in infinite fluid.

3. A better approximation to K''_D has been given by Rosenhead (Ref. 29) by adopting an empirical value for the extent of annihilation of the vorticity. This can be written as

$$K''_D = \frac{4a}{d} \coth \frac{\pi a}{b} \left[\frac{U_1}{U} - 2\left\{ 2(1-h) - \coth \frac{\pi a}{b} \times \left(\frac{3a}{c} + \frac{b(1-K)}{a\pi} \right\} \left(\frac{U_1}{U} \right)^2 \right] \qquad \ldots\ldots (70)$$

where

$$h = \frac{c}{a} \frac{\cosh \frac{\pi a}{b}}{\sinh \frac{\pi c}{2b} + \sinh \frac{\pi a}{b}}$$

$$K = \frac{4\pi c}{b} \frac{\cosh^2 \frac{\pi a}{b}}{\left(\sinh \frac{\pi c}{b} + \sinh \frac{\pi a}{b} \right)^2} - \frac{\pi c}{2b} \left\{ \frac{1}{\sinh^2 \frac{\pi (c+a)}{2b}} - \frac{1}{\cosh^2 \frac{\pi (c-a)}{2b}} \right\}$$

and

U_1 = velocity of vortices in the rear of the body

provided $\frac{b}{c} \leqq 0.815$.

4. For a flat plate equation (70) gives results in closer agreement to those obtained experimentally. If however U_1 is written in equation (69) instead of U, Glauert's equation gives results closely in agreement to the experimental results than by the use of $\cancel{U}$ u in (69). Hence it was decided to use U_1 in equation (68),(69) which is now

$$K''_D = K_D + 32 \frac{a}{d} \frac{a}{c} \left(\frac{U_1}{U}\right)^2 \qquad \ldots (71)$$

It is seen from either (70) or (71) that to find K''_D it is necessary to find $\frac{a}{d}$, $\frac{b}{c}$, and $\frac{U_1}{U}$ experimentally.

As mentioned in Part VII the writer has been unable to obtain these particulars for $\frac{d}{2c} = \frac{1}{2}$ for reasons mentioned there.

experimentally?

5. Rosenhead and Schwabe (Ref. 30) have however given these particulars for a wide range of values of $\frac{d}{2c}$. These have been used by the writer to evaluate K''_D by using (71), instead of (70) since $\frac{b}{c}$ is not generally less than 0.815, which is the necessary condition for using (70).

The values of K_D for use in equation (71) have been obtained from the experiments of Relf (Ref. 33) and of Wieselbarger (Ref. 34).

The values of K''_D and K'_D along with other particulars from Rosenhead and Schwabe's experiments are given in Table (XIII).

Figure (35) shows K''_D plotted on $\frac{d}{2c}$ for four different values of Reynold's number. This figure also includes the values of K''_D for $\frac{d}{2c} = \frac{1}{2}$ and $\frac{d}{2c} = 0.3$ as obtained by the writer in Part V. From this figure it is seen that the assumption made in this part of the paper is legitimate.

6. Figure (36) shows $\frac{K''_D}{K_D}$ plotted ~~on~~ against $\frac{d}{2c}$ and $\frac{K''_D}{K_D}$ can be expressed by the following approximate equation for Reynold's number higher than 80.

$$\frac{K''_D}{K_D} = 1 + 2\left[\frac{0.09}{\left(1-\frac{d}{2c}\right)^2} + \frac{0.22}{\left(1-\frac{d}{2c}\right)} - 0.31\right] + \left[\frac{0.09}{\left(1-\frac{d}{2c}\right)^2} + \frac{0.22}{\left(1-\frac{d}{2c}\right)} - 0.31\right]^2$$

$$\frac{K''_D}{K_D} = \left[\left\{\frac{0.09}{\left(1-\frac{d}{2c}\right)^2} + \frac{0.22}{\left(1-\frac{d}{2c}\right)} - 0.31\right\} + 1\right]^2 \qquad \text{......} \ (72)$$

Figure (37) shows $\frac{K''_D}{K_D}$ for $\frac{d}{2c} = 0.5$ and $\frac{d}{2c} = 0.3$ as obtained in the present experiments plotted ~~on~~ against $\log_{10} R$. It is seen from this figure that no simple ~~law holds~~ relation connect~~ing~~s $\frac{K''_D}{K_D}$ and R.

PART IX.

DRAG OF GRID.

1. Drag forces on a single cylinder of the grid or of a cylinder between channel walls can be obtained from the approximate expression (72), which holds for $R \geqq 80$

$$\text{Drag} = K''_D \, e \, d \, l \, U^2 \qquad \text{.........} \quad (73)$$

Substituting the value of $\frac{K''_D}{K_D}$ ~~for~~ from (72)

$$\text{Drag} \doteqdot K_D \, e \, d \, l \, U^2 \left[1 + 2 \left\{ \frac{0.09}{\left(1-\frac{d}{2c}\right)^2} + \frac{0.22}{\left(1-\frac{d}{2c}\right)} - 0.31 \right\} + \left\{ \frac{0.09}{\left(1-\frac{d}{2c}\right)^2} + \frac{0.22}{\left(1-\frac{d}{2c}\right)} - 0.31 \right\}^2 \right]$$

$$\text{Drag} \doteqdot K_D \, e \, d \, l \, U^2 \left[\left\{ \frac{0.09}{\left(1-\frac{d}{2c}\right)^2} + \frac{0.22}{\left(1-\frac{d}{2c}\right)} - 0.31 \right\} + 1 \right]^2$$

for $R > 80$. .... (74)

2. A rig~~id~~orous? form of (74) would be obtained by introducing the parameter R in the equation (74), as can be seen from Fig. (37). But it is almost impossible to give a simple expression to allow for variations of $\frac{K''_D}{K_D}$ with Reynold's number.

For a grid $\frac{d}{2c} = \frac{1}{2}$, and $\frac{d}{2c} = 0.3$, the drag forces can be calculated by reading off K''_D from Figures (31) and (32).

3. At low Reynold's number the velocity distribution in the channel tends to become parabolic and as such some sort of corrections are necessary to find K''_D from the observed K''_D given in Figure (31) for use in equation (73). (See Part XI).

PART X.

METHOD OF CORRECTING THE VELOCITY DUE TO CHANNEL WALL CONSTRICTION.

1. A method of correcting for the increased velocity of flow past cylinder due to the presence of the channel walls based on perfect fluid motion has been given in Part I. General methods of correcting this effect, applicable to bodies of different shapes have been given by Lamb (Ref. 35), Watson (Ref. 31), and Lock and ~~Johanson~~ Johansen (Ref. 37).

2. An alternative way of ~~looking at~~ estimating the increase in velocity is to take regard the increased total drag coefficient at any Reynolds number as being ~~caused by~~ proportional to the increased velocity squared. Thus increased velocity $U+\Delta U$ is given by

$$\frac{U+\Delta U}{U} = \sqrt{\frac{K''_D}{K_D}} \qquad \text{.......... (75)}$$

The values of $\frac{\Delta U}{U}$ are given in Tables (X), (XII), and (XIII) for different values of $\frac{d}{2c}$.

3. These are shown plotted in Fig. (38) on approx. $\frac{d}{2c}$. Except at low Reynolds number ($\lessapprox$ 80) the relation between ~~law connecting~~ $\frac{\Delta U}{U}$ + $d/2c$ can be approximately expressed as

$$\frac{\Delta U}{U} = \frac{0.09}{\left(1-\frac{d}{2c}\right)^2} + \frac{0.22}{\left(1-\frac{d}{2c}\right)} - 0.31 \qquad \text{...... (76)}$$

4. A more general form of (76) would be obtained by allowing for variation of $\frac{\Delta U}{U}$ with Reynold's number.

5. Figure (39) shows $\frac{\Delta U}{U}$ for $\frac{d}{2c} = \frac{1}{2}$, ~~and~~ 0.3, plotted ~~on~~ against $\log_{10} R$.

PART XI.

APPROXIMATE ESTIMATE OF K''_D FOR A SINGLE CYLINDER IN A STREAM WITH PARABOLIC DISTRIBUTION OF VELOCITY.

1. From the preceding parts of the paper the drag coefficients K''_D for a cylinder between channel walls having uniform velocity distribution is known. An approximate method of estimating ~~for~~ the increase in the drag coefficient due to parabolic velocity distribution in the same channel is based on ~~obtained by finding~~ determining the average velocity of the fluid meeting the cylinder. If U'' be this velocity and U the average velocity in the channel, then it is easily found that

$$\frac{U''}{U} = \frac{1}{2}\left(3 - \frac{d^2}{4c^2}\right) \qquad \text{........... (77)}$$

Let K'''_D be the drag coefficient of the cylinder in parabolic stream then

$$\frac{K'''_D}{K''_D} = \frac{1}{4}\left(3 - \frac{d^2}{4c^2}\right)^2 \qquad \text{........ (78)}$$

These are evaluated for different values of $\frac{d}{2c}$ and are given in Table (XIV). It is seen that when $\frac{d}{2c} = 1$, ? $\frac{K_D}{K''_D}$ is 1.00. This may appear anomalous, but this is not so, because in such a case the average velocity of fluid meeting the cylinder is the same as the average velocity of the channel

$\frac{K'''_D}{K''_D}$ are shown plotted in Figure (40).

Part XII.

CONCLUSION.

A summary of the results is given at the beginning of the paper. The ~~f~~ Flow past Grid (also the flow past a cylinder in between parallel channel walls) differ~~s~~ from that of Flow past a Single Cylinder in infinite field in the following ways:-

(i) The drag coefficients K_D'' K_P and K_V for a cylinder of the Grid is higher than those for a single cylinder.

(ii) The formation of Stationary eddy pair behind the cylinder of a Grid ~~is~~ takes place at a higher Reynold's Number than that behind a single cylinder.

(iii) The formation of the Karman Street Vortices is also delayed in the case of the Grid.

(iv) The front generator pressure of cylinder of the Grid appears to be slightly different from that of a single cylinder.

The major portion of the ~~is paper~~ work of this paper has been carried out with the D.S.I.R. maintenance allowance and the work has been completed with the Carnegie Research Scholarship The writer wishes to express his indebtedness to these authorities

The work has been carried out in the James Watt Engineering Laboratories of the Glasgow University, under the direction of Professor J.D.Cormack ,Director of Laboratories, and the writer wishes to thank him for advice, guidance and facilities given to him.

To Dr.Thom the writer is indebted for the loan of the detailed solution for Single Cylinder in infinite field, as referred to in the Part II of the paper, and also for help and advice throughout.

References.

(I) H.Lamb:- On the Reflection and Transmission of Electric Waves of Metallic Grating : Proc.Lomd.Math.Soc. vol 29 pp 523-44 (1897-98).

(2) W.Page:- Some Two Dimensional Problems in Electrostatics and Hydrodynamics: Proc.Lond.Math.Soc.vol II 2nd series pp/313-23 (1912-13)

(3) J.Leathem:- Some Applications of Conformal Transformation to Problems in Hydrodynamics: Phil.Trans.Roy.Soc. Sec A vol 215 pp439-88 (1915)

(4) W.Bickley:- Two Dimensional Problem concerning Single Closed Boundary: Phil.Trans.Roy.Soc.,Sec A vol 228 (1928)

(5) K.Ochiai:- A Note on a Potential Problem: Proc.Phys.Math.Soc. Japan.,3rd Series,vol 12,No I pp 6-8 (1930)

(6) Müller:- Mathematische Strömungslehre pp 80-83.

(7) R.Richter:- Einfluss der Lochung von Transformatorkernen auf den Magnetisierungsstrom: E and M Heft 20 (May 1933)

(8) L.Bairstow and F.Berry:- Two Dimensional Solutions of Poisson's and Laplace's equations: Proc.Roy.Soc.,Sec A vol 95 pp 457-~~99~~ 75 (1919)

(9) A.Thom:- An Investigation of Fluid Flow in Two Dimensions: R and M. 1194 (Nov.1928)

(10) H.Winny:- Graphical Solutions for Inviscid Fluid: R and M 1473 (April 1932)

(11) A.Thom and J.Orr:- The Solution of the Torsion Problem for Circular Shafts of Varying Radius: Proc.Roy.Soc.,Sec A vol 131 pp 30-37 (1931).

(I2) A.Thom:- The Flow past Circular Cylinders at Low Speeds: Proc.Roy.Soc.,Sec A.vol I4I pp65I-69 (I933)

(I3) A.Thom:- Aeronautical Research Committee: F.M. IOI (I933)

(I4) Oseen:- Uber die Stokes'sche Formel und uber eine verwandte Aufgabe in der Hydrodynamik: Arkiv fur Mathematik..... Bd VI no 29 (I9IO)

Lamb's Hydrodynamics p 574 ,5th.edtn (I930)

(I5) L.Filon:- The Second Approximation to Oseen Solution for Motion of a Viscous Fluid.: Phil.Trans.Roy.Soc., Sec A vol 227 pp 92-I35 (I928)

(I6) Lamb:- Hydrodynamics: pp 582-83 5th edtn (I930)

(I7) Bairstow, Cave and Lang:- The Resistance of a Cylinder in Viscous Fluid : Phil.Trans.Roy.Soc.,Sec A vol I23 p 383 (I923)

(I8) Bairstow, Cave and Lang:- The Two Dimensional Slow Motion of Viscous Fluids: Proc.Roy.Soc.,Sec A p 394-4I3 (I922) vol IOO

(I9) L.Bairstow:- Skin Friction: Journal Roy.Ae.Soc.,pI (Jan I925)

(20) S.Goldstein:- Concerning some Solutions of the Boundary Layer Equations in Hydrodynamics: Proc.Camb.Phil.Soc.,vol XXVI Part I (I929)

(2I) V.Falkner and S.Skan:- Approximate Solutions of the Boundary Layer Equations: R and M I3I4 (April I930)

(22) A.Thom:- Boundary Layer of the Front Portion of a Cylinder: R and M II76 (July I928)

(23) J.Green:- Viscous Layer associated with Circular Cylinder: R and M I3I3 (April I930)

(24) W.Linke:- Neue Messungen zur Aerodynamik des Zylinders, insbesondere seines reinen Reibungswiderstandes: Dissertation ,Leipzig (I93I)

(25) A.Thom:- The Pressure on the Front Generator of a Cylinder R and M I389 (Dec I930)

(26) S.Sengupta:- Flow round Curved Channel : Paper III of the present thesis.

(27) L.Rosenhead:- Systems of Double Row of line Vortices in a Channel of Finite Breadth where the Axis of the Row is parallel to the Axis of the Channel: Proc.Camb. Phil.Soc., vol 25 p277 (I928-29)

(28) L.Rosenhead:- Double Row of Vortices with Arbitrary Stagger: Proc.Camb.Phil.Soc.,vol 25 p I32 (I928-29)

(29) L.Rosenhead:- The Karman Street Vortices in a Channel of Finite Breadth: Phil.Trans.Roy.Soc.,Sec A p 275 vol 228 (I929)

(30) L.Rosenhead and M.Schwabe:- The Experimental Investigation of the Flow behind Circular Cylinders in Channels of Finite Breadths: Proc.Roy.Soc.,Sec A vol I29 pp II5-35 (I930)

(3I) L.Rosenhead:- The Spread of Vorticity in the Wake behind a Cylinder: Proc.Roy.Soc.,Sec A vol I27 pp590-6I2 (I930)

(32) H.Glauert:- The Characteristics of a Karman Street in a Channel of Finite Breadth: Proc.Roy.Soc.,Sec A vol I20 p 34 (I928) also R and M II5I (I927)

(33) E.Relf:- Discussion of the Results of Measurements of Resistance of Wires, with some additional tests on the

on the Resistance of Wires of Small Diameters : Tech.Report, Adv. Cmttee for Aeronautics , p 47 (I92I)

(34) A.Wieselberger:- Neuere Festellungen uber die Gesetze des Fluss and Luftwiderstandes: Physik.Zeitschr. vol 22 pp 32I-28 (I92I)

(35) H.Lamb:- On the Effect of Walls of an Experimental Tank on the Resistance of a Model: R and M IOIO.

(36) G.Watson:- The Use of Series of Bessel Functions in Problems connected with Cylindrical Wind Tunnels; Proc.Roy.Soc., Sec A vol I30 p29 (I930)

(37) C.Lock and F.Johansen:- Wind Tunnel Interference on Stream line Bodies., R and M I45I (June I93I)

---------- -------- ----------

Table I.

$\frac{d}{2c}$	$\frac{d^1}{2c}$	$\frac{d}{2c} - \frac{d^1}{2c}$	$\frac{d^1}{d}$
$\frac{2}{3}$	0.6370	0.0297	0.955
$\frac{1}{2}$	0.4926	0.0074	0.987
$\frac{3}{10}$	0.2988	0.0012	0.997

Table II.

ξ	θ°	$\frac{d}{2c} = \frac{1}{2}$		$\frac{d}{2c} = \frac{2}{3}$	
		q	p_1	q	p_1
2	0	0	+1	0	+1
$1\frac{3}{4}$	29.0	1.160	-0.345	1.272	-0.62
$1\frac{1}{2}$	40.3	1.579	-1.491	1.825	-2.32
1	60.0	2.203	-3.853	2.620	-5.84
0	90.0	2.712	-6.389	3.580	-11.80
Angle at which $p = 0$		$p = 0$, $\theta = 25^{\circ}\ 15'$		$p = 0$, $\theta = 22^{\circ}\ 24'$	

Table III.

Hole diameter	$\frac{d}{2c}$	Experiments.			Theory	Remarks
		Resistance in ohms.	Increase in Resistance in ohms.	n.	n	
0	0	0.001578	0	0	0	
0.125	0.124	0.001592	0.000014	0.0291	-	
0.250	0.247	0.001621	0.000043	0.0896	-	
-	0.300	-	-	-	0.1513	from (5)
0.500	0.494	0.001808	0.000230	0.4791	-	
-	0.500	-	-	-	0.4807	from approximate solution.
-	$0.\dot{6}66$	-	-	-	0.9930	from (5)

Table IV.

$\frac{d}{2c}$	$\frac{\Delta U}{U}$ from (26)	$\frac{\Delta U}{U}$ from (28)	Remarks.
0.05	-	0.005	from (3)
0.10	-	0.017	"
0.20	-	0.017	"
0.30	-	0.081	from (7)
0.50	-	0.272	"
0.50	0.309	0.356	Arithmetical solution.
$0.6\dot{6}$	0.677	0.790	"
$0.6\dot{6}$	-	0.652	from (7)

Table V.

ξ	θ°	ζ_{o}	$\frac{p - p_o}{\frac{1}{2}\rho U^2}$
+2	0	0	+1.386
$+1\frac{3}{4}$	29.0	3.60	+0.302
$+1\frac{1}{2}$	40.3	4.40	-0.430
+1	60.0	4.00	-2.620
0	90.0	2.00	-4.630
-1	120.0	0.80	-4.330
$-1\frac{1}{2}$	139.7	0.40	-3.870
$-1\frac{3}{4}$	151.0	0.06	-3.850
-2	180.0	0	-3.780

Table VI.

θ	p_1	$dp_1/d\theta$	$\sqrt{1-p_1}$	$h = \frac{-1}{2\sqrt{1-p_1}}\frac{dp_1}{d\theta}$	$\frac{3}{2}\frac{\sqrt{1-p_1}}{h^2}\frac{dh}{d\theta}$	$\sqrt{Uh/r\nu}$
10°	0·870	-1·048	0·361	1·452	0·427	39·4
20°	0·561	-2·307	0·663	1·743	0·191	43·1
30°	0·043	-3·615	0·980	1·845	-0·923	44·5
40°	-0·707	-5·800	1·308	2·218	-2·44	48·8
50°	-1·718	-3·807	1·650	1·153	-4·43	35·1
60°	-2·305	-2·692	1·820	0·739	-5·50	28·2

θ	x =	0	0,I	0,2	0,3	0,4	0
For all Values of θ	$F_1'(x)$ =	0,866	0,939	I,032	I,I54	I,3I6	I
	$F_1(x)$ =	0	0,088	0,I88	0,296	0,420	0
	$\int x\, F_1'(x)\, dx$ =	0	0,0045	0,0I92	0,046	0,092	0
	$f_1(x)$ =	0	0,005	0,0I9	0,040	0,072	0
	M =	0,26	0,26	0,26	0,25	0,24	0
	$f_2(x)$ =	0	0,009I	0,036	0,077	0,I28	0
	$\int_x^{10} f_2(x)\, dx$ =	0,I45	0,I44	0,I42	0,I36	0,I26	0
	$x^3 - 3x + 2$ =	2,00	I,70I	I,408	I,I20	0,864	0
10°		~~0,04I~~	~~-0,04I~~	~~-0,040~~	~~-0,039~~	~~-0,036~~	~~-0~~
	$\frac{2}{3}N$ =	-0,04I	-0,04I	-0,040	-0,039	-0,036	-0
	$F_2'(x)$ =	0,826	0,893	0,967	I,069	I,I97	I
	$F_2(x)$ =	0	0,086	0,I79	0,28I	0,394	0
	n (mm) =	0	0,022	0,045	0,07I	0,I00	0
	q cm/sec.	0	0,296	0,592	0,888	I,I84	I
20°	$\frac{2}{3}N$ =	-0,0I8	-0,0I8	-0,0I8	-0,0I7	-0,0I6	-0
	$F_2'(x)$ =	0,820	0,884	0,958	I,057	I,I76	I
	$F_2(x)$ =	0	0,085	0,I77	0,278	0,389	0
	n (mm) =	0	0,020	0,04I	0,064	0,093	0
	q cm/sec =	0	0,544	I,088	I,632	2,I76	2
30°	$\frac{2}{3}N$ =	0,090	0,089	0,087	0,084	0,078	0
	$F_2'(x)$ =	0,794	0,849	0,9I4	I,003	I,III	I
	$F_2(x)$ =	0	0,082	0,I70	0,266	0,372	0
	n (mm) =	0	0,0I8	0,038	0,060	0,084	0
	q cm/sec =	0	0,805	I,6I0	2,4I5	3,220	4
40°	$\frac{2}{3}N$ =	0,236	0,235	0,230	0,220	0,206	0
	$F_2'(x)$ =	0,758	0,807	0,864	0,940	I,030	I
	$F_2(x)$ =	0	0,078	0,I62	0,252	0,35I	0
	n (mm) =	0	0,0I6	0,033	0,052	0,072	0
	q cm/sec =	0	I,076	2,I50	3,225	4,300	5
50°	$\frac{2}{3}N$ =	0,429	0,426	0,420	0,402	0,372	0
	$F_2'(x)$ =	0,7I7	0,76I	0,807	0,872	0,95I	I
	$F_2(x)$ =	0	0,074	0,I52	0,236	0,328	0
	n (mm) =	0	0,02I	0,043	0,067	0,093	0
	q cm/sec =	0	I,352	2,704	4,056	5,408	6
60°	$\frac{2}{3}N$ =	0,53I	0,528	0,520	0,498	0,462	0
	$F_2'(x)$ =	0,700	0,739	0,782	0,840	0,9I4	I
	$F_2(x)$ =	0	0,072	0,I48	0,229	0,3I7	0
	n (mm) =	0	0,026	0,052	0,08I	0,II2	0
	q cm/sec =	0	I,493	2,986	4,479	5,972	7

Table VIII.

R	C in $(1+\frac{C}{R})\frac{1}{2}\rho U^2$
189	6.62
197	7.60
220	7.04
230	9.20
417	8.54
457	9.14
628	8.64
809	10.8
20	7.72 - from Part II
-	9.52 - Perfect flow $\frac{d}{2c} = \frac{1}{2}$
-	10.52 - " " $\frac{d}{2c} = \frac{2}{3}$

Table IX.

OIL (I)	OIL (2)	OIL (3)
R = 7,9	R = I8,9	R = 25,6
d = 0,635cm	d = I,266cm	d = I,266cm
U = 4,93 cm/sec	U = 4,79 cm/sec	U = 8,3 cm/sec
ν = 0,396 c.g.s.	ν = 0,320 c.g.s.	ν = 0,4I0 c.g.s.
$\Delta\theta$ = 4 degrees	$\Delta\theta$ = 4 degrees	$\Delta\theta$ = 4 degrees

$\theta - \Delta\theta$	p_I (I)	p_I (2)	p_I (3)
0	I,520	I,300	I,234
36	- 0,245	- 0,366	-0,450
76	- 2,96	- 2,64	- 3,00
II6	- 6,I6	- 4,79	- 4,0I
I56	- 5,84	- 4,I0	- 3,50
I80	- 5,84	- 4,I0	- 3,48

WATER (4)	WATER (5)	WATER (6)
R = 58	R = 7I	R = I55
d = 0,3I75 cm	d = 0,3I75 cm	d = 0,3I75 cm
U = 2,0 cm/sec	U = 2,4 cm/sec	U = 5,2 cm/sec
$\Delta\theta$ = 2 degrees	$\Delta\theta$ = 2 degrees	$\Delta\theta$ = 2 degrees

0	I,I5	I,I5	I,06
I8	0,88	0,77	0,57
38	- 0,06	- 0,I3	- 0,66
58	- I,38	- I,47	- 2,37
78	- 2,45	- 2,53	- 3,89
98	- 2,70	- 2,84	- 4,29
II8	- 2,46	- 2,66	- 3,85
I38	- 2,06	- 2,48	- 3,58
I58	- 2,23	- 2,33	- 3,48
I80	- 2,23	- 2,3I	- 3,43

WATER (7)	WATER (8)	WATER (9)
R = I89	R = I9I	R = I94
d = 0,3I75cm	d = 0,3I75cm	d = 0,3I75cm
U = 6,5cm/sec	U = 6,8cm/sec	U = 7,Icm/sec
$\Delta\theta$ = 2 degrees	$\Delta\theta$ = 2 degrees	$\Delta\theta$ = 2 degrees

0	I,05	I,04	I,04
8	0,95	0,97	0,97
28	0,23	0,26	0,26
48	- I,23	- I,28	- I,27
68	- 2,78	- 3,05	- 2,84
88	- 3,77	- 4,03	- 3,88
I08	- 3,77	- 3,97	-3 ,75
i28	- 3,32	- 3,52	- 3,28
I48	- 3,24	- 3,34	- 3,I7
I68	- 3,06	- 3,32	- 3,I2
I80	- 3,06	- 3,32	- 3,I2

$$p_I = (p - p_0) / \tfrac{1}{2}\rho U^2$$

Table Ix (Contd)

$p_1 = (p - p_0) / \frac{1}{2} \rho U^2$

WATER
d = 0,3I75 cm
$\Delta\, \theta$ = 2 degrees

θ - Δθ	p_1	p_1	θ - Δθ	p_1
(IO)	(IO) R = 220 U = 7,762cm/sec	(II) R = 229 U = 8,5 cm/sec	(I2) R = 230 U = 8,I cm/sec	(I2)
0	I,04	I,04	0	I,04
8	0,94	0,95	I8	0,7I
28	0,I5	0,I8	38	- 0,32
48	- I,33	- I,20	58	- I,88
68	- 2,89	- 2,72	78	- 3,I9
88	- 3,83	- 3,69	98	-3 ,54
I08	- 3,68	- 3,62	II8	- 3,I6
I28	- 3,24	- 3,23	I38	- 2,87
I48	- 3,I7	- 3,02	I58	- 2,8I
I68	- 3,I5	- 2,94	I80	- 2,82
I80	- 3,I4	- 2,94		

WATER
d = 0,6347 cm
0 = 4 degrees

θ - Δθ	p_1	θ - Δθ	p_1
(I3) R = 295 U = 5,4 cm/sec		(I4) R = 457 U = 7,98 cm/sec	
0	I,03	0	I,02
5	0,99	I5	0,7I
25	0,25	35	- 0,36
45	- I,26	55	- I,75
65	- 2,86	75	- 2,59
85	- 3,79	95	- 2,44
I05	- 3,50	II5	- 2,I8
I25	- 3,28	I35	- 2,I7
I45	- 2,69	I55	- 2,I9
I65	- 3,I9	I80	- 2,I9
I80	- 3,I0		

Table IX (Contd)

$p_1 = (p - p_0) / \frac{1}{2}\rho U^2$

WATER
d = I,2659 cm
$\Delta\theta$ = 4 degrees

$\theta - \Delta\theta$	p_1	p_1	p_1
	(I5) R = 4I7 U = 3,99 cm/sec	(I6) R = 573 U = 5,3 cm/sec	(I7) R = 837 U = 7,6 cm/sec
0	I,02	I,0I	I,0I
23	0,36	0,I7	0,36
43	-I,I7	-I,I0	-0,88
63	-2,7I	-2,50	-2,36
83	-3,I9	-3,00	-2,75
I03	-2,76	-2,5I	-2,36
I23	-2,43	-2,32	-2,I9
I43	-2,46	-2,44	-2,I9
I63	-2,46	-2,42	-2,I9
I80	-2,46	-2,42	-2,I9

$\theta - \Delta\theta$	p_1	p_1	p_1
	(I8) R = 628 U = 5,6 cm/sec	(I9) R = 800 U = 7,8 cm/sec	(20) R = 85I U = 8,3 cm/sec
0	I,0I	I,0I	I,0I
6	0,94	0,92	0,96
26	0,20	0,20	0,27
46	- I,27	- I,25	- I,38
66	- 2,64	- 2,70	- 2,55
86	- 3,0I	- 3,09	- 3,I5
I06	- 2,52	- 2,62	- 2,75
I26	- 2,4I	- 2,55	- 2,68
I46	- 2,43	- 2,55	- 2,66
I66	- 2,43	- 2,56	- 2,66
I80	- 2,43	- 2,56	- 2,66

Table IX (Contd)
Pressure Drag Coefficients

R	K_P^*	Note
7,9	2,99	OIL
I8,9	I,96	,,
25,6	I,57	,,
58	I,07	WATER
7I	I,I5	,,
I55	I,44	,,
I89	I,37	,,
I9I	I,47	,,
I94	I,37	,,
220	I,36	,,
229	I,32	,,
230	I,26	,,
295	I,27	,,
4I7	0,96	,,
457	0,92	,,
573	0,93	,,
628	I,02	,,
837	0,98	,,
809	I,06	,,
85I	I,00	,,

Table X

$d = 0{\cdot}6324$ cm , $l = 3{\cdot}835$ cms

R	K_D''	K_D'' / K_D	$\Delta U/U$
Experiments in Oil			
0,93	2I,I3	3,98	0,99
I,37	2I,53	5,58	I,36
2,08	I4,59	4,7I	I,I7
2,2I	I2,95	4,46	I,II
3,59	7,96	3,62	0,9I
3,66	8,I7	3,7I	0,93
4,03	8,02	3,82	0,95
4,94	5,86	3,22	0,80
5,20	5,89	3,37	0,84
Experiments in Water			
II2	I,64	2,34	0,53
I59	I,66	2,52	0,58
209	-- I,54	2,37	0,54
229	I,46	2,28	0,5I
257	I,38	2,I9	0,48

Table X (Contd)

Cylinder dia = I,2598 cm , length = 3,873 cm

R	K_D''	K_D''/K_D	$\Delta U/U$
Experiments in Oil			
2,45	I5,I7	5,52	I,35
3,49	I0,54	5,I3	I,27
4,63	8,83	5,02	I,24
5,69	9,4I	5,54	I,36
6,97	5,78	3,6I	0,90
7,I3	5,40	3,57	0,89
8,83	4,49	3,26	0,80
9,47	4,29	3,30	0,8I
I2,42	3,37	2,8I	0,68
Experiments in Water			
I2,2	3,30	2,75	0,66
I7,0	2,75	2,60	0,6I
22,0	2,5I	2,64	0,62
32,0	2,0I	2,30	0,52
56,8	I,78	2,27	0,5I
87,3	I,65	2,28	0,5I
95,0	I,60	2,24	0,50
295	I,32	2,26	0,50
339	I,20	2,00	0,42
398	I,I5	I,98	0,4I
437	I,I0	2,00	0,42
50I	I,03	I,87	0,37
525	0,99	I,83	0,37
562	I,06	I,98	0,4I
66I	I,I3	2,I5	0,46
759	I,09	2,I8	0,48
955	I,I2	2,26	0,50

Table XI

R	K_D''	R	K_D''
	0,316 cm dia Cylinder		
75	I,55	I56	I,06
82	I,7I	I68	I,I3
87	I,72	I70	I,I4
94	I,58	I9I	I,27
I04	I,54	2I3	I,I8
I36	I,I0	225	I,33
I40	I,02	246	I,36
I52	I,II		
	0,632 cm dia Cylinder		
2II	I,I5	40I	I,22
25I	I,28	405	I,06
3I4	I,3I	434	I,33
329	I,08	442	I,09
340	I,28	506	I,03
395	0,98		
	I,254 cm dia Cylinder		
526	0,99	807	I,30
565	I,0I	824	I,23
567	I,I4	860	I,24
635	I,23	885	I,I9
664	I,I9	964	I,35
766	I,08	986	I,29

Note:- All Experiments done in Water.

Table XII $d/2c = 0,3$

R	K_D''	K_D''/K_D	$\Delta U/U$
Cylinder dia 0,6324 cm , length 3,835cm			
191	1,16	1,78	0,33
288	0,870	1,43	0,20
339	0,89	1,48	0,22
407	0,76	1,31	0,15
457	0,72	1,30	0,14
479	0,77	1,40	0,18
501	0,74	1,35	0,16
Cylinder dia 1,2598cm length 3,873 cm			
503	0,79	1,43	0,20
581	0,73	1,37	0,17
671	0,79	1,51	0,23
760	0,77	1,54	0,24
818	0,74	1,49	0,22
863	0,79	1,57	0,25
1058	0,72	1,48	0,22
1138	0,78	1,65	0,28

Note:- All Experiments done in Water.

Table XIII

d/2c	R	U_I/U	a/d	a/c	$K_D'' - K_D$	K_D''	K_D''/K_D	$\Delta U/U$
0,060	82	0,05	0,9	0,I08	0,0078	0,738	I,0I	0,006
0,098	78	0,08	I,3	0,255	0,0679	0,798	I,09	0,046
,,	82	0,08	I,2	0,235	0,0578	0,783	I,08	0,040
0,I92	49	0,06	0,9	0,345	0,034I	0,834	I,04	0,020
,,	57	0,07	0,8	0,307	0,0385	0,8I4	I,05	0,025
,,	90	0,05	0,7	0,269	0,0I49	0,725	I,02	0,020
,,	I68	0,I2	0,7	0,269	0,0854	0,725	I,I3	0,064
0,333	I09	0,I6	0,6	0,400	0,I966	0,862	I,30	0,I39
,,	I75	0,I3	0,6	0,400	0,I297	0,770	I,20	0,096
,,	325	0,I8	0,6	0,400	0,2489	0,859	I,4I	0,I85
0,667	I02	0,46	0,45	0,600	I,828I	2,5I3	3,67	0,9I5
,,	207	0,54	0,5	0,667	3,III7	3,742	5,94	I,437
,,	386	0,55	0,4	0,534	2,0683	2,64I	4,59	I,I42
,,	750	0,52	0,5	0,667	2,8853	3,386	6,77	I,502

Table XIV.

$\frac{d}{2c}$	$\frac{K'''_D}{K''_D}$
0	2.250
$\frac{1}{10}$	2.236
$\frac{1}{3}$	2.086
$\frac{1}{2}$	1.891
$\frac{10}{15}$	1.633
$\frac{9}{10}$	1.99
1	1.000

List of Tables.

List of Diagrams.

666

List of Plates.

LOSSES AT SUDDEN ENLARGEMENT AND CONTRACTION IN TWO DIMENSIONS.

List of Symbols (Paper II)

h_1	= Distance between walls in narrow channel
h_2	= ,, ,, ,, wide ,,
B	= Depth of channel
r	= h_1/h_2
n_1	= Couette correction for enlargement
n_2	= ,, ,, ,, contraction
m_1	= Kinetic Energy correction factor in enlargement
m_2	= ,, ,, ,, ,, contraction.
n	= $n_1 + n_2$
m	= m_1 (for viscometry)
u_1	= Average velocity in the narrow channel v
ρ_1, μ_1	= Density and Viscosity of fluid
p_e	= pressure ~~correc-~~ loss in enlargement
p_e'	= ,, ,, ,, contraction.
R	= Reynold's Number.

LOSSES AT SUDDEN ENLARGEMENT AND CONTRACTION IN TWO DIMENSIONS.

SUMMARY:-

(1) Part I of this paper gives an expression for the end correction, which might be used in viscometry by flow between parallel plates.

(2) Part II gives the arithmetical solution of flow at sudden enlargement and sudden contraction for infinitely low Reynold's Number. The end correction n is found to be 0,322.

(3) The arithmetical solution at R=20,25 is given. The values of n (the Couette correction) and that of m (the factor of the Kinetic energy term) are found to be 0,322 and 1,022 respectively.

(4) A stationary eddy is found to be developed at each corner.

(5) Part III deals with the experiments and gives support to the theoretical values of n and m in enlargement and contraction.

(6) Values of n and m are given for use in the theoretical formula for viscometry.

(7) It is shown that probably below R = 145 periodic eddies are not shed from the enlargement.

(8) Appendix I gives experimental verification of Poiseuille's ~~Law~~ Equation for a ratio (B/h)=25 and also shows the effect

on measurements of pressure drop, when one of the gauge points is near the disturbed region.

(9) Appendix II gives a solution for $\nabla^2\psi = 0$, for the enlargement ratio r = 4. Increment in the electrical resistance of a similar conducting sheet of uniform thickness is found. The good agreement found with the results of ~~existing mathematical~~ numerical method of solution is ~~supplies~~ a ~~justification~~ verification of the latter. ~~arithmetical method of solution used.~~

Part I.

The steady motion of incompressible viscous fluid between two stationary parallel plates of infinite width is given by (Ref. 1).

$$u = -\frac{1}{2\mu} z(h-z)\frac{\partial p}{\partial x}$$
$$= \frac{1}{2\mu} z(h-z)\frac{p}{l} \qquad \ldots\ldots\ldots\ldots\ldots\ldots (1)$$

where

u = velocity in the x-direction

v = w = 0, velocities in y and z directions

z = distance from one of the planes, taken as the x-y plane of reference

h = distance between the planes

ρ, μ are the density and the viscosity of the liquid

p = drop in pressure over a length l along x

and $\frac{\partial p}{\partial x}$ constant along x axis p/l.

Unit width of the plane is considered. The quantity of fluid passing per second through each section (h x l) is therefore

$$Q = \int_0^h u\, dz = \frac{h^3}{12\mu}\frac{p}{l} \qquad \ldots\ldots\ldots\ldots\ldots\ldots (2)$$

It is seen that the distance h between the planes enters into the equation (2) to the third power. Hence, the distance h does not need to be measured with quite so high an accuracy as is needed for the determination of the diameter of the capillary tube which enters to the fourth power in the absolute determination of viscosity by means of capillary tubing. This suggests the use of flow between parallel plates for the measurement of viscosity. Further, there is the possible advantage of securing more uniformity of distance between the plates than that of the diameter in the case of capillary tubes. The surface can be ground with precision and examined.

If Q is measured and the pressure difference between two points unaffected by the entry and the exit conditions, are measured, then μ can be determined from equation (2).

Appendix I of this paper shows that this ~~law~~ relation holds within experimental accuracy, for a ratio (B/h) = 25, where B is the depth of the channel. Flow through pipes of rectangular section has been investigated for a wide range of the ratio B/h, from 2,92 to 169,3 (Ref. 2, 3, 4). For a low ratio of B/h the following ~~law~~ relation holds (Ref. 4) and can be used,

$$Q = -\frac{Bh^3}{12\mu}\left(\frac{\partial p}{\partial z}\right)\left\{1 - \frac{192}{\pi^5}\left(\tanh\frac{\pi B}{2h} + \frac{1}{3^5}\tanh\frac{3\pi B}{2h} + \cdots\right)\right\}$$

.... (3)

The usual practice of viscometry is to use a capillary tube attached to a wide reservoir, and to time a measured quantity/

quantity of discharge. The same method can be adopted for parallel plates if similar correction terms are determined. One of the objects of the present investigation is to determine these corrections.

A good discussion of the nature of these corrections for a capillary tube has been given in Dr. Guy Barr's "Monograph of viscometry" (Ref. 5).

The liquid must enter the capillary tube or channel in a converging stream from the wider supply vessel. This involves a loss of pressure and the necessary correction to Poiseuille's Equation Law goes by the name of Couette, who first suggested it. This is done by the hypothetical addition of ($n_{\ddagger}$ x d) to the length of the tube, where n is a numerical nondimensional factor and d is the diameter. The corresponding Couette Correction in two dimensional case is given by (n_2.h).

The liquid when discharging from the exit end of the channel or tube similarly diverges and requires an additional correction n_e x h.

Dr. W. N. Bond (Ref. 6) has given a method of viscosity determination with short tubes and orifices. The value of n as experimentally determined by Dr. Bond has been found to be in good agreement with that obtained by arithmetical solution of the equations of viscous flow at sudden enlargement in pipes by Dr.

A/

A. Thom (Ref. 7). Dr. Thom's paper was available to the writer in its rough proof and the first portion of the Part II of this paper, dealing with the solution of $\nabla^4\psi = 0$, was undertaken at his suggestion.

In addition to this correction to the length a further correction is required at higher Reynold('s) number for the extra energy carried away by the emergent fluid.

This energy is dissipated in ~~the form of heat due to~~ eddy formation and ultimately as heat. This correction is usually applied ~~by using~~ as a ~~correction~~ factor m, to the energy of the liquid ~~existing~~ in the portion of the channel where the flow is governed by Poiseuille's Law.

Kinetic energy imparted to the liquid is retained by the liquid until it leaves the channel and is equal to the sum of the kinetic energies of the elements of the liquid which passes any cross section per second. (For tubes see Ref. 5)

Volume of liquid passing through dz, = u dz. Kinetic energy of this volume element passing per unit time is

$$\frac{1}{2}\rho\,(u\,dz)\,u^2 \qquad \text{.................. (4)}$$

Kinetic energy ~~of the liquid flowing through~~ carried across the whole cross section per second is therefore

$$K.E./\text{sec} = \frac{1}{2}\rho\int_0^h u^3\,dz$$

$$= \frac{1}{2}\rho\,\frac{1}{8}\left(\frac{p}{l\mu}\right)^3\frac{1}{140}\,h^7 \qquad \text{.................. (5)}$$

Substituting the value of $\left(\frac{p}{l\mu}\right)$ from equation (2) in equation (5) we get,

$$K.E/_{sec} = \frac{27}{35}\, e\, \frac{Q^3}{h^2} \quad \text{................ (6)}$$

The kinetic energy /per sec. carried away by the emergent liquid is therefore

$$KE/_{sec} = m\, \frac{27}{35}\, e\, \frac{Q^3}{h^2} \quad \text{................ (7)}$$

The total rate of work done ~~per second~~ must be equal to the rate of work done against the viscous forces plus the kinetic energy /per sec of the carried by the liquid ~~when it~~ out of leaves the channel.

The rate of work done against the viscous forces is therefore ~~(per sec)~~

$$= p \int u\, dz \; - \; m\, \frac{27}{35}\, e\, \frac{Q^3}{h^2}$$

$$= pQ - m\, \frac{27}{35}\, e\, \frac{Q^3}{h^2} \quad \text{................ (8)}$$

Hence the pressure (p_1) effective in overcoming viscous resistance is given by

$$p_1 = p - m\, \frac{27}{35}\, e\, \frac{Q^2}{h^2} \quad \text{................ (9)}$$

adventitious →

additional → ~~Due to~~ on account of the end effects we have of walls ~~now~~ an effective length of $(l + nh)$ where $n = n_1 + n_2$

Thus

$$Q = \frac{h^3}{12\mu}\, \frac{p_1}{(l+nh)} \quad \text{................ (10)}$$

Substituting for p_1 from equation (9) in equation (10) we get

$$\mu = \frac{p h^3}{12 Q (l + nh)} - m \frac{q}{140} \frac{e Q h}{(l + nh)}$$

.... (11)

Equation (11) ~~now~~ gives the necessary formula for the determination of μ , with parallel plates, corresponding to that with capillary tubes.

Parts II and III of this paper give values of n and m to be used in applying equation (11) to viscometric purposes.

Part II.

The problem of steady viscous flow between two parallel planes of infinite width, originally at a distance of 8 units, the distance suddenly enlarging to 32 units is solved for low Reynold's Number by the use of a method due to Dr. Thom (Refs. 7, 8, 9, 10).

The general equations of steady two dimensional viscous flow reduce to

$$\left.\begin{aligned} \nu \nabla^2 \xi &= u \frac{\partial \xi}{\partial x} + w \frac{\partial \xi}{\partial z} \\ \text{where} \quad \nabla^2 \psi &\equiv 2\xi = \frac{\partial w}{\partial x} - \frac{\partial u}{\partial z} \\ \text{and} \quad u = -\frac{\partial \psi}{\partial z} &, \quad w = \frac{\partial \psi}{\partial x} \end{aligned}\right\} \qquad \text{............. (12)}$$

The method of solution of equation (12) is one of repeated interpolation in a field of initially assumed values of ξ and ψ. The field is divided into squares of side 2n and the values of are assumed for each corner. These assumed values for corners give ξ_c and ψ_c for the centre of the square, ~~when~~ using the following interpolation formulae ~~are used~~.

$$\xi_c = \xi_M - \frac{1}{16\nu}\left\{(a-c)(B-D) + (b-d)(C-A)\right\} \qquad \text{............. (13)}$$

$$\psi_c = \psi_M - n^2 \xi_c \qquad \text{............. (14)}$$

where,

$$\psi_M = (A + B + C + D) \div 4 \qquad \ldots\ldots\ldots\ldots (15)$$

$$\xi_M = (a + b + c + d) \div 4 \qquad \ldots\ldots\ldots\ldots (16)$$

and A, B, C, D are the corner values of ψ and a, b, c, and d are the corresponding values of ξ.

Having used equations (13) and (14) to find the values at the centres of all squares they are used again to find new value at the original corners. The process is repeated till all the values over the field have settled. At solid boundaries the value of ξ_S on the surface are obtained from the approximate expression.

$$\xi_S = (\psi_G - \psi_S) \div m_3^2 \qquad \ldots\ldots\ldots\ldots (17)$$

where ψ_S value of ψ on surface and ψ_G value of ψ at a point G distant m_3 from the surface.

The process involving the repeated use of formulae (13) to (16) in conjunction with (17) has been found to be convergent, provided the squares used are not too large (Refs. 7, 8, 9, 10).

The spacing of the stream lines between the parallel walls beyond the region of the enlargement are calculated for the two portions of the channel and the stream lines are roughly sketched.

The field is now divided into suitable squares and ξ and ψ values are assigned to the corners. Repeated use of the formulae

(13) to (17) is made till the field is settled.

At first it was assumed that viscosity was indefinitely great that is, $\nabla^4\psi \to 0$, so that the equation (13) now simplifies to

$$\xi_c = \xi_M \qquad \text{............ (18)}$$

This enables the use of various speeding up processes, some of which have been communicated to the Aeronautical Research Committee by Dr. Thom (Ref. 11).

The difficulties of the regressive intruding corner and a method of overcoming them ~~this~~ have been stated mentioned by Dr. Thom (Refs. 7, 11). The corner is enlarged several times and the size of the squares reduced. Although the vorticity at the corner is probably infinite, the errors have little effect on the rest of the field, provided sufficient enlargement is made. The corner is separated out by dotted lines and the rest of the field is treated and settled. Then the values near the corner are modified as affected by the change in the field outside.

The important part of the field $\nabla^4\psi = 0$, as solved, is shown in Fig. (1). The figures on the top of a corner of a square give the ξ value and the bottom figure the ψ value.

The figure (2) shows the stream lines corresponding to this solution, and Fig. (3) shows the contours of vorticity.

The/

The formula necessary for calculating the pressure distribution can be derived from the fundamental hydrodynamical equations of viscous flow. (Ref. 8) The pressure along a line parallel to the x-axis is given by

$$p_A + \frac{1}{2}\rho q_A^2 = p_B + \frac{1}{2}\rho q_B^2 + 2\rho\nu\int_A^B \frac{\partial\xi}{\partial z}\,dx - 2\rho\int_A^B w\xi\,dx \qquad (19)$$

where

$$q^2 = u^2 + w^2$$

In calculating the pressure difference between such points A, B for $\nabla^4\psi = 0$, the following reasoning is employed. (Ref. 7) Since the viscosity has been assumed infinite, it is evident that infinite pressure will be necessary to cause motion. (Hence, it is necessary to think of viscosity as large but not infinite.) Equation (19) then simplifies to

$$p_A - p_B = 2\rho\nu\int_A^B \frac{\partial\xi}{\partial z}\,dx \qquad (20)$$

The values of ξ are known in the entire field and $\frac{\partial\xi}{\partial z}$ is found by numerical differentiation by the Gregory-Newton Formula (Ref. 12). Figure (4) shows $\frac{\partial\xi}{\partial z}$ along z = h/2, i.e. the median.

The pressure loss is calculated by evaluating the integral $2\rho\nu\int_A^B \frac{\partial\xi}{\partial z}\,dx$ along the median by careful mechanical integration. The pressure loss for sudden enlargement is found to be the same as that which would take place with an additional length of (0,322/

(0,322 x h) of the small channel.

At zero Reynold's number the solution for the flow in the reverse direction is exactly identical and so gives the same equivalent increase in the length of the small channel.

Thus at low Reynold's Number the value of n giving the corrections for contraction and enlargement together is 0,<u>644</u>, this figure is of the same order as (1,132) for tubes as found by Dr. Bond (Ref. <u>6</u>) experimentally and of (2 x 0,588) as determined by Dr. Thom (Ref. 7) by the above arithmetical method. Dr. Bond's experiments indicate that up to Reynold's Number 10, n is constant. It is suggested that this figure (n = 0,644) can be taken for channels up to Reynold's Number 5, along with m = 0 for use in equation (11).

Section II.

Dr. Thom has shown that this method of solution is capable of showing ~~up~~ stationary eddies behind cylinders (Ref. 10). As a point of interest and also with a view to determining a value of m in equation (11) theoretically, the solution has been repeated for Reynold's Number 20,25. Equations (13) to (17) are used with γ = 12,25 giving the above value of R.

Starting with the figures obtained from the R = 0 solution, the above formulae are applied hundreds of times till only small variations movements are obtained. Figure (5) shows part of the field, and Figure/

Figure (6) shows the stream lines obtained.

Both figures (5) and (6) show a stationary eddy at the corner. It is possible that such an eddy exists as in the case of cylinders. It has been shown by Davies and White (Ref. 2) that below R = 140, all disturbances are damped down. Hence periodic eddies are not shed from the enlargement below R = 140. But this does not preclude the formation of stationary eddies as obtained arithmetically.

Farren (Ref. 13) has demonstrated the periodic eddies as they develop and detach themselves by smoke photographs. These are shown in Plate I. The shape of the eddy here obtained seems to be different from that obtained by Farren. But this is not surprising, when the nature of the Kidney eddies and Karman Street vortices are considered.

Figure (7) shows the velocity profile at various sections for R = 20,25 as obtained in the solution.

The pressure drop between two points A and B on the undisturbed parts of the two channels is calculated by using equation (19) which reduce to

$$p_A + \frac{1}{2} \rho u_A^2 = p_B + \frac{1}{2} \rho u_B^2 + 2\rho\nu \int_A^B \frac{\partial \xi}{\partial z} \, dx \qquad \ldots\ldots\ldots\ldots\ldots (21)$$

But $u_B = ru_A$, where $r = h_1/h_2$ and h_1 and h_2 are the distances between the channel walls in the two parts. Then

$$p_A - p_B = \frac{9}{8} \rho u_1^2 (r^2 - 1) + 2\rho\nu \int_A^B \frac{\partial \xi}{\partial z} dx \qquad \text{.......... (22)}$$

where u_1 is the average velocity in the narrow channel and is two thirds of the maximum velocity U_A.

The term $2\rho\nu \int_A^B \frac{\partial \xi}{\partial z} dx$ then gives the total loss in pressure due to viscosity and kinetic energy.

The term involving the kinetic energies in the two channels would remain the same if the flow althrough in the two channels were laminar. But in that case there would have been some viscous loss as given by equation (1). If l_1 and l_2 are the distances of the points A and B from the enlargement, respectively, and $\left(\frac{\partial p}{\partial x}\right)_1$ and $\left(\frac{\partial p}{\partial x}\right)_2$ are the pressure gradients in the two channels, then such viscous loss is given by

$$\left(\frac{\partial p}{\partial x}\right)_1 l_1 + \left(\frac{\partial p}{\partial x}\right)_2 l_2 \qquad \text{.......... (23)}$$

Hence, the extra ~~loss~~ pressure drop caused by the enlargement is given by

$$p_e = 2\rho\nu \int_A^B \frac{\partial \xi}{\partial z} dx - \left\{ \left(\frac{\partial p}{\partial x}\right)_1 l_1 + \left(\frac{\partial p}{\partial x}\right)_2 l_2 \right\} \qquad \text{.......... (24)}$$

This loss includes the ~~pressure drop~~ pressure drop term due to divergence of the emergent jet and the excess of energy per sec. over that ~~given by~~ implied in Poiseulle's ~~Law,~~ Equation carried away by the emerging liquid.

The ~~loss~~ pressure drop p_e is now expressed in terms of the pressure ~~loss~~ drop in the narrow channel, ~~as~~ given by Poiseulle's ~~Law~~ Equation, by the following/

following equation,

$$p_e = \frac{12\mu Q}{h_1^3} N_1 h_1 \qquad \text{..........} \; (25)$$

i.e., $N_1 h_1$, gives the additional length to be added to the channel.

Figure (8) shows $\frac{\partial \xi}{\partial z}$ along x, $\frac{\partial \xi}{\partial z}$ being obtained by numerical differentiation as before. $2e\gamma \int_A^B \frac{\partial \xi}{\partial z}\, dx$ is now obtained by careful mechanical integration. N_1 is found to be 0,351.

This extra pressure loss as indicated before is due to the additional length $\cancel{N_1}\, n_1 h_1$ (divergence loss) and to the excess energy loss $(m-1)\frac{27}{35} e \frac{Q^2}{h_1^2}$ Hence

$$p_e = \frac{12\mu Q\, n_1 h_1}{h_1^3} + (m-1)\frac{27}{35} e \frac{Q^2}{h_1^2} \qquad \text{..........} \; (26)$$

Now equating the expressions on the left of equations (25) and (26) we get

$$\frac{12\mu Q N_1}{h_1^2} = \frac{12\mu Q\, n_1}{h_1^2} + (m-1)\frac{27}{35} e \frac{Q^2}{h_1^2} \qquad \text{..........} \; (27)$$

Hence

$$N_1 = n_1 + (m-1)\frac{9}{140} R \qquad \text{..........} \; (28)$$

where R = Reynolds Number = $\frac{u_1 h_1 e}{\mu}$

$\cancel{N_1}$ as found above is 0,351. Assuming that the effect of divergence is the same at all Reynolds Number, i.e., $\cancel{N_1}\, n_1$ = 0,322 m_1 is found to be 1,022 from equation (28), but this value of m_1 ~~however~~ will not apply to contraction.

The value ~~of~~ m_1 (1,022) ~~as found~~ for enlargement in

channels/

channels compares well with the figure m=1,08 for tube viscometry ~~as~~ given by Schiller (Ref. 5, 14) from the hydrodynamical theoretical considerations and from his weighted mean of experimental results.

Part III of this paper gives experimental confirmation of the values of n and m.

Part III.

Method of Reduction

Theory of Experiments:-

Substitute for $2e\gamma \int_A^B \frac{\partial \xi}{\partial z}\,dx$ from equation (24) in equation (28) the following equation is obtained

$$p_e = p_A - p_B + \frac{9}{8} \rho u_1^2 (1 - r^2) - \left\{ \left(\frac{\partial p}{\partial x}\right)_1 l_1 + \left(\frac{\partial p}{\partial x}\right)_2 l_2 \right\}$$

.... (29)

This equation gives a method of determining p_e, the enlargement pressure drop losses, provided the difference of pressure $(p_A - p_B)$ on the median of the channel, the pressure gradients, and the average velocity are shown. If the gauge points are situated far enough away from the disturbed portion of the channel then $(p_A - p_B)$ will be the same as that obtained from observations at the corresponding points on the walls of the channels. And $\left(\frac{\partial p}{\partial x}\right)_1$ and $\left(\frac{\partial p}{\partial x}\right)_2$ can either be calculated from equation (2) or deduced from measurements of pressure drop along the undisturbed parts of the channels.

p_e can now be expressed according to the equation (25) and N_1 found. Then using equation (28) n_1 and m_1 can be found.

The corresponding expression for pressure losses in sudden contraction is similarly

$$p_e' = p_A - p_B - \frac{9}{8} \rho u_1^2 (1 - r^2) - \left\{ \left(\frac{\partial p}{\partial x}\right)_1 l_1 + \left(\frac{\partial p}{\partial x}\right)_2 l_2 \right\}$$

.... (30)

and m_2 and n_2 can be found by using equations (25) and (28) as before.

<u>Experiments</u>:-

The sketch of the apparatus used is given in Figure (9). It was arranged so that the distance between the plates could be adjusted. The apparatus consists of four similar pieces of brass plates, three inches wide and 3/4" thick with a flange. These pieces are bolted together. The top and bottom are closed by means of thick rubber insertion held secure by two 1/4" thick brass plates screwed down. The ends are also similarly closed. These cover plates and end plates are all slotted to allow for adjustment. The two flanges are first bolted giving the required enlargement ratio and the distances between them are measured with a microscope. The top and bottom plates are then fixed. Pressure measurements in the narrow section give a check to the measurement of the distance h when water or any liquid of known viscosity is used.

There are 46 pressure holes of diameter 0,014". ~~These~~ connect to the pressure box as shown. The apparatus is supplied from a constant head reservoir and discharges through the jacket of the pressure box into a glass tube. This end of the discharge pipe is kept submerged in the water in a glass tube and the level in the glass tube is kept adjusted to a fixed mark. Any variation of this level indicates a change in the rate of flow. At low speed it is impossible to adjust the flow with valves. Different constant speeds were obtained by fitting nozzles of different diameters at the exit end. The pressure box is used to avoid ~~an~~ error due to temperature changes. Thermometers are fixed at the inlet/

inlet and the outlet. Two holes are provided for sucking out any air in the apparatus. The pressure differences are measured by a sensitive Tilting Gauge (Ref. 15). The average velocity is measured by timing the discharge from the outlet required to fill a graduated cylinder.

The flow is reversed and the effect of a sudden contraction is studied.

The dimensions as measured are given below

h_1 = 0,3034 cm. (direct measurement) 0,304 cm. (from pressure measurements)

h_2 = 1,209 cm., B = 7,597 cm.

Ratio of B/h = 25

Enlargement ratio = h_2/h_1 3,98.

The coefficient of viscosity is taken from standard Tables (Ref. 16).

The results of experiments are shown in Table I and II for enlargement and contraction respectively.

Figure (10) shows the variation of pressure along the wall of the channel for enlargement. The corresponding figure for contraction is the Figure (11).

Figure (11) shows a region of high pressure at contraction as is to be expected, since these points are on the walls near the contraction, where the liquid comes to rest.

Table III gives the maximum excess of pressure, from the smooth/

smooth curve which is probably the curve of pressure variation along the median of the channel. Figure (12) shows this excess pressure plotted on Reynold's Number.

Figure (13) shows p_e and N_1 for enlargement against ~~on a base of~~ R. For reasons mentioned later the points above R = 145 cannot be used for the calculation of n_1 and m_1. (on account of ~~Due to~~ eddying)

Figure (14) shows p_e' and N_2 for contraction. The flow in the wide channel approaching the section is probably not laminar and hence Figure (14) shows scattered points, and ~~as such~~ the values of m_2 and n_2 can be taken as approximate only.

Results.

For sudden enlargement n_1 and m_1 are found to be 0,33 and 1,01 respectively. These compare well with the values 0,322 and 1,022 as obtained from the numerical ~~theoretical~~ solutions. ~~given.~~

For sudden contraction n_2 and m_2 are found to be 0,400 and 0,680 respectively.

Bond's experiments for tubes (Ref. 6) indicate that up to R = 10, n is constant and m = 0. Above this n tends to vanish and m tends to unity. Bond's value of n for both enlargement and contraction is 1,132.

The present experiments for channels gives n_1 and m_1 as constant for enlargement as is to be expected from the theory, whereas for contraction n_2 seems to increase for high Reynold's Number. It must however be mentioned that the results of the contraction experiments/

experiments are liable to error owing to possible turbulence in the enlarged part of the channel.

For use for viscometric purposes the values of n and m to be taken are 0,644 and 1,022, respectively. Since the fluid in the wide supply vessel is more or less stationary, m_2 is not to be taken into account in equation (11).

Thus equation (11) now is

$$\mu = \frac{p h^3}{12 Q (l + 0.644h)} - 1.022 \left(\frac{9}{140} \frac{\rho Q h}{l + 0.644h} \right) \qquad \text{........... (31)}$$

Another interesting result obtained is the Reynold's Number at which eddies (periodic) are first shed from the enlargement. The eddies as shed travel down the wide channel. A graduated capillary tube was fitted on to a hole on the enlarged channel. The level of water is seen to oscillate as the eddies travel down. The frequency and the maximum amplitude of oscillation were observed and these are shown in Tables IV and V. The frequency and the amplitude both increase with Reynold's Number. Figure (15) shows these plotted on Reynold's Number. From the oscillation experiments it is seen that probably at R = 145 the periodic eddies are first shed. Below R = 145 these eddies are probably damped down. The experiments of Davies and White (Ref. 2) indicate that below R = 140 the effect of entrant conditions is probably damped down and below this value of R the flow is always stable. The present experiments support this view. And as/

as seen, it is likely that below R = 140 no periodic eddies are shed, although a stationary eddy probably exists at each corner as shown in Figures (5) and (6) of Part II.

Appendix I.

Equation The verification of the equation (2), i.e. Poiseuille's Law is given here, for B/h 25. Table VI gives $F/\rho v^2$ for different values of Reynold's Number $\frac{\rho v h}{\mu}$. Figure (16) shows log. $F/\rho v^2$ plotted against $\log_{10} R$.

It is seen that the experimental points lie on the theoretical line given by Poiseuille's equations Law up to Reynold's Number 183. Beyond this the experimental points lie above this line. This is due to one of the gauge points being near the entry, as is also seen from the experiments of Davies and White (Ref.2). That this is so is confirmed from the Figure (17) in which L/h (where L is the distance of the gauge point) is plotted against R. The value of L/h lies on this curve as given by Davies and White.

The experiments on frequency and amplitude of oscillation due to eddies indicate that below R = 145, disturbances do not travel down, stream thus lend support to Davies and White's result (R = 140) as obtained from the Figure (17). Hence it is probably ~~quite~~ right to assume that below R = 140, the motion is always stable, as stated ~~proposed~~ by Davies and White.

Appendix II.

It has been shown by Dr. Thom (Ref. 10) that the use of the method indicated in Part II for solution of viscous fluid motion is considerably facilitated if a conformal grid is used in the case of curved boundaries. The same applies to the ~~intrud-~~ regressive corners.

This involves an initial solution of $\nabla^2\psi = 0$. This can be done by Schwarzian Transformations. The writer's attention was drawn by Dr. B. Hague to the fact that the corresponding electrical problem has been solved by many writers (Refs. 19, 20, 21). Thus C. H. Lees obtains the same transformation as given by

$$z = 2A\left\{ \begin{matrix} \tanh^{-1} \\ \coth^{-1} \end{matrix} \pm \sqrt{\frac{t+a}{t+1}} - \frac{1}{\sqrt{a}} \begin{matrix} \tanh^{-1} \\ \coth^{-1} \end{matrix} \sqrt{\frac{t+a}{a(t+1)}} \right\} \qquad \text{..........} \; (32)$$

$$w = C \log t \qquad \text{..........} \; (33)$$

$\nabla^2\psi = 0$ for this problem has also been ~~done~~ evaluated by the arithmetical method, indicated in Part II.

Figure (18) shows this solution and Figure (19) the stream lines. The equipotential lines are not shown.

This solution is used to find the increase in electrical resistance of a conducting sheet of uniform thickness, due to sudden enlargement, for an enlargement ratio of 4.

Flow/

Flow of electric current along a sheet is analogous to that of irrotational motion in hydrodynamic. The analogy has been extended by G. I. Taylor (Ref. 22) to cases of compressible fluids.

If $t = \rho\sigma$, then $V = \phi$, $W = \psi$; when

$$\left.\begin{aligned} \frac{\partial\psi}{\partial x} &= \rho v , \quad \frac{\partial\psi}{\partial z} = -\rho u \\ \frac{\partial\phi}{\partial x} &= -u , \quad \frac{\partial\phi}{\partial z} = -v \\ \frac{\partial\psi}{\partial z} &= -tf = \frac{t}{\sigma}\frac{\partial V}{\partial x} \end{aligned}\right\} \qquad \ldots\ldots\ldots\ldots\ldots (34)$$

Where. $V =$ Electric potential function

$W =$ Electric Current function

$t =$ thickness.

$\sigma =$ Specific. Resistance.

If now A and B are two points far away from the disturbed region, then drop of potential between A and B can be calculated by integrating $\frac{\partial\psi}{\partial z}$ along AB, since

$$\int_A^B \frac{\partial\psi}{\partial z}\,dx = \rho\int_A^B \frac{\partial\phi}{\partial x}\,dx. \qquad \ldots\ldots\ldots\ldots\ldots (35)$$

$\frac{\partial\psi}{\partial z}$ is obtained by careful mumerical differentiation and the drop in potential is evaluated by mechanical integration.

Figure/

Figure (20) shows $\frac{\partial \psi}{\partial z}$ plotted on x
And the increase in resistance is due to 0,690 x h, where h is the width of the narrow part of the sheet. This compares well with the figure 0,650 as given by C. H. Lees (Ref. 19) for the enlargement ratio of 4.

Appendix III.

In the above experiments, the flow cannot be considered as strictly two dimensional and as such it is necessary to examine how far this affects the equation (29) used in deducing the experimental results. The maximum velocity in the narrow channel from formula corresponding to equation (3)

$$\doteqdot \frac{3}{2} u_1$$

The maximum velocity in the wide channel is

$$\doteqdot 0.9998\left(\frac{3}{2} u_2\right) = 0.9998 \left(\frac{3}{2} \cdot \tfrac{1}{4} u_1\right)$$

Hence the kinetic energy term in equation (29) is hardly affected.

Pressure gradients $\left(\frac{\partial p}{\partial x}\right)_1$, $\left(\frac{\partial p}{\partial x}\right)_2$ have also to be corrected if these are calculated from equation (2). ~~Then~~ Thus for narrow channel

$$\left(\frac{\partial p}{\partial x}\right)_1 \doteqdot \left(\frac{1}{0.975}\right)\left(\frac{12 \mu Q}{h_1^3}\right)$$

And for the wide channel

$$\left(\frac{\partial p}{\partial x}\right)_2 \doteqdot \left(\frac{1}{0.900}\right)\left(\frac{12 \mu Q}{h_2^3}\right)$$

In conclusion the writer wishes to express his indebtedness to the Department of Scientific and Industrial Research for the grant of a Maintenance allowance, which enabled him to carry out this work along with others. The writer also wishes to thank Professor J. D. Cormack, the Director of the James Watt Engineering Laboratories of the Glasgow University, where the work was carried out, for advice and for the facilities given to him. He is also indebted to Dr. A. Thom for generous help and advice throughout.

Table I.

R	p_e	N_1
17,98	0,098	0,345
33,8	0,191	0,366
59,7	0,371	0,399
81,2	0,557	0,427
115,6	0,903	0,476
132,0	1,042	0,500
234,6	2,350	0,596
305,9	3,540	0,690

Table II.

R	p_e^1	N_2
18,3	0,140	0,466
72,4	-1,500	-1,23
183,0	-6,74	-2,24
237,0	-20,07	-5,17
303,8	-37,72	-7,60
385,9	-63,33	-10,00
469,3	-94,95	-12,20

Table III.

R	Excess pressure Chattock Turns over mean curve.
18,30	0,20
32,61	0,40
48,68	0,58
72,40	1,10
117,30	2,00

Table IV.

R	Frequency of Oscillation due to eddies.
199,5	0,91
228,9	0,85
258,2	0,91
317,0	1,00
381,5	1,00
457,8	1,20
548,1	1,36
551,7	1,30

Table V.

R	Maximum Amplitude of oscillation due to eddies
156,2	0,015 cm.
199,5	0,020 "
275,8	0,030 "
289,9	0,050 "
381,5	0,300 "
397,9	0,300 "
423,7	0,450 "
474,2	0,600 "
501,2	0,600 "
536,4	0,700 "
569,3	0,800 "
581,1	0,800 "

Table VI.

R	F/ev^2	R	F/ev^2
18,20	0,335	117,5	0,053
32,36	0,180	163,2	0,038
47,86	0,128	234,4	0,028
48,98	0,128	269,2	0,027
72,44	0,084	309,0	0,023
75,86	0,078	316,2	0,024
81,28	0,073	354,8	0,020
112,20	0,058	467,7	0,017

REFERENCES.

(1) Lamb - Hydrodynamics, pp. 550-1, 5th edition, (1930) C.U.P.

(2) Davies and White - Pro. Roy. Soc., Sec. A, 119, pp. 92-107 (1928).

(3) Fromm - Z.f.ang. Math. Mech., vol. 3, p. 339, (1923).

(4) Cornish - Proc. Roy. Soc., Sec. A, 120, pp. 691-700, (1928).

(5) Barr - Monograph of Viscometry, Chaps. I, II, (1930) Ox. U.P.

(6) Bond - Proc. Phys. Soc. vol. 34, pp. 139-144 (1921-22).
vol. 33, pp. 225-230 (1921).

(7) Thom - Ae. Research. Ctte., R.M. 1475, (1932).

(8) Thom and Orr - Proc. Roy. Soc. Sec. A, vol. 141 pp. 30-37 (1931).

(9) Thom - R.M. 1194 (1929).

(10) Thom - Proc. Roy. Soc., Sec. A, vol. 141, pp. 651-669 (1933).

(11) Thom - Ae. Research, Ctte., F.M. 101, (1933).

(12) Whittaker and Robinson - The Calculas of Observation Arts 35-36, 2nd edition, (1929) Blackie.

(13) Farren - J. Roy. Ae. Soc., vol. XXXVI, ~~pp.~~ , June 1932, p. 464 (~~1932~~).

(14) Schiller - Forschungs Arbeiten, V.D.I., (1922) No. 248.

(15) Thom - R.M. 1389 (1930).

(16) Landolt und Bornstein - Phys. Chem. Tabellen, p. 288, Zweite Auflage (1894) Springer.

(17) Lees - Phil. Mag., S 6, vol. 16, Nov. (1908) pp. 734-739.

(18) Cramp and Calderwood - J. Inst. Elect. Eng. vol. 61, p. 1061 (1923).

(19) Carter - J.I.E. Eng., vol. 64, p. 1115 (1926).

(20) Weber - Archiv. f. Elect. Tech., vol. 17, p. 174 (1927).

(21) Taylor and Sharman - Proc. Roy. Soc., Sec. A, vol. 121, pp. 194-217 (1928).

List of Tables.

List of Diagrams.

α

List of Plate.

FLOW IN A SEMICIRCULAR BEND OF A CHANNEL OF RECTANGULAR SECTION.

List of Symbols.

V	Mean Velocity of Channel
ρ, μ	Density and Viscosity of Fluid
R	Reynold's Number
D	Mean dia of coil
d	Pipe diameter
H	Channel width
a	Radius of the inner channel wall
m	Hydraulic Mean Depth.

FLOW IN A SEMICIRCULAR BEND OF A CHANNEL OF RECTANGULAR SECTION.

Summary.

In the first part the paper gives a summary of the more important investigation on the flow of fluid through curved passages as published by other investigators.

In the writer's experiments four different stages are observed to exist, these being

(I) Stage during which the internal circulation is absent.

(II) Stage during which the bottom circulation only is important.

(III) Stage during which the top circulation is prominent.

(IV) Beyond the critical speed, a stage during which the top circulation appears to exist.

The critical velocity for the bend is found to be less than that in the straight portion of the channel.

The paper proposes a criterion for the transition of flow from (I) to stage (II) for curved tubes.

A confirmation of James Thomson's Theory of Meanderings of Rivers in alluvial plains is shown.

In the second part of the paper an arithmetical solution of $\nabla^2\psi = 0$ for this curved passage is given and similarity of the flow pattern for irrotational motion and very viscous flow is discussed.

INTRODUCTION.

This investigation has been carried out in the James Watt Engineering Laboratories of the Glasgow University under the ~~directions~~ direction of Professor J. D. Cormack.

The problem of the effects of curvature on the flow of fluids has received ~~frequent~~ much ~~attentions~~ attention. The flow of fluids in a curved open topped channel of rectangular section with free, upper surface is of special interest because of its engineering applications. The phenomenon of the meanderings of rivers in alluvial plains has been explained through studies of flow in a curved channel by Professor James Thomson. (Ref. 1).

Recently, an oil and water channel had been constructed in this laboratory for the study of various Hydrodynamical problems at low Reynold's number. The channel in its present shape is shown diagrammatically in Fig. (1), the old channel has been described in full by Dr. A. Thom. (Ref. 2).

It was thought that an investigation of the nature of the flow in the curved portion of the channel was necessary to understand the probable effects of using a semicircular bend as an entrance to or an exit from the straight portion of the channel, which forms the working section.

Part I of this paper deals with the nature of the flow in the curved path and also includes a summary of the available information on the subject.

Part II of this paper gives an arithmetical solution of the flow for this bend for perfect fluid.

General Survey.

A comprehensive survey is beyond the scope of this paper, but a brief outline of certain essential points is thought necessary for the proper comprehension.

Professor James Thomson (Ref. 1) has explained the cause of protection of the convex bank of the river, from the erosive action, thus: The water near the concave bank accelerates itself on account of due to the centrifugal force; whereas near the convex bank it does not do so. This gives rise to cross gradient of the free level across the section, rising up from the convex to the concave bank. The water adjacent to the bed of the channel is least affected by the centrifugal force due to viscous effects and tends to rise up between the convex bend and the streamlines. The net effect is the scouring of the concave bank and the protection of the inner bank. There is further protection due to the deposition of silt carried by the water from the concave to the convex bank.

! adjective

The current engineering idea (Ref. 3) about the flow pattern across the section is shown in Fig. (2) which is for 90^{0} in a semicircular bend.

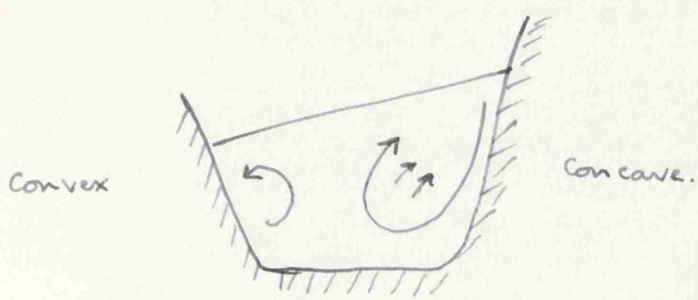

FIG 2

Gibson further states that the linear speed at the concave bank is greater than that at the convex bank and during the flooding period when erosion is maximum, the scouring action is further intensified ~~due~~ by to the impact of water on the concave bank.

The other investigations of flow in curved channel during steady motion are those of Eustice (Refs. 4, 5, 6, 7) and of Hinderks (Ref. 8). Both these observers and others have noticed spiral vortices. A physical explanation of this double spiral flow has been given by Eustice for pipes.

The case of a tube of circular section bent into an anchor ring has been dealt with mathematically by W. R. Dean. The cross pressure gradient produced by the centrifugal force, sets up an internal circulation, Fig. (3) ~~indicates the nature of circulation~~, as given by W. R. Dean (Ref. 9) in his diagram showing the path of a particle in the plane of cross section.

Convex 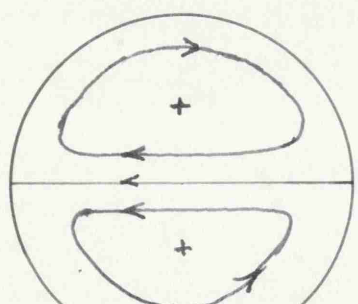 con cave.

FIG 3

Such a path has been indicated by J. Eustice (Ref. 5) and experimentally demonstrated by G. I. Taylor (Ref. 11). The second paper of W. R. Dean (Ref. 10) gives a mathematical form in which the pressure losses in a curved pipe may be expressed. This is different from the Reynold's Criterion which is used as abscissa for plotting pressure drops in straight path. C. M. White (Ref. 12) has given experimental verification of Dean's theory, which shows that for curved pipes (according to notation used by C. M. White).

$$\frac{F}{\rho V^2} = \frac{\rho V d}{\mu} = \frac{Fd}{\mu V} = f\left[\frac{\rho V d}{\mu}\cdot\left(\frac{d}{D}\right)^{\frac{1}{2}}\right] \quad \ldots\ldots\ldots (1)$$

where F is the resistance.
V " mean velocity.
d " diam. of the pipe.
D " diam. of the coil.

This expression on the right hand side ~~$f\left[\frac{\rho V d}{\mu}\left(\frac{d}{D}\right)^{\frac{1}{2}}\right]$~~ is called by Mr. C. M. White Dean's Criterion.

The case of pure two dimensional flow (or at any rate of the flow through a curved rectangular tube has been investigated by the German workers (Ref, 13, and 15) from the point of view of the effects of centrifugal force on the boundary layers associated with the concave and convex surfaces. Dr. J. W. Maccoll's paper (Ref. 13) gives a physical interpretation of the comparative thickening of the boundary layer on the concave side to that of the convex side, in the light of Prandtl's theory.

W. R. Dean (Ref. 16) has also deduced mathematically a Criterion ~~to find out~~ for the Reynold's number at which transition to turbulent flow takes place in the case of flow under pressure through the annular space formed by two coaxial cylinders, the flow being in the plane of cross section. This will be discussed later on in the paper.

This more or less gives a survey of the field covered. A comprehensive bibliography is given in the Bulletin (Ref. 14) mentioned.

It was felt that although sufficient data exist for curved pipes - the available data for curved channels are comparatively small. Further, the flow in a channel should be intermediate between that of purely two-dimensional cases and that of three-dimensional cases like that of a pipe, because of the existence of the bottom of the channel and of the free water surface. A double helical flow should exist even in the case of a channel.

It is shown in this paper that the existence of the free surfaces in the case of a curved channel introduces complexity. The cross gradient of the water surface set up by the centrifugal force plays a dominating part in the internal circulation. Although some writers (Ref. 17) seem to think that this transverse inclination is only noticed in small experimental channels due to cross strain; it has been however shown that in the case of the Mississipi river the difference of elevation on two sides of a bend during flood may amount to as much as one foot (Ref. 18).

EXPERIMENTS.

The experiments consist of photographing of coloured fluid filaments ~~lines~~ and fixing their positions in three dimensions.

The channel used is substantially ~~essentially~~ the same as that employed and described in full by Dr. A. Thom (Ref. 2). It has been however lengthened to get over the surging effects otherwise felt at the bend near the propeller. The inlet end to the working section is now of rectangular shape as compared to the original semicircular end. Fig. (1) shows the channel. The length of the straight portion is now 84" as compared to 42" previously.
The water is circulated by a small propeller driven by a $\frac{1}{4}$ H.P. D.C. Shunt Motor through belt drive. Guide vanes are used at the right angled bends. Previously 90° circular arcs were tried as guide vanes. Now 105° adjustable vanes are used. These seem to give a more uniform flow in the working portion of the channel. Three sets of honey-comb, one $2\frac{1}{2}$" wide with 100 cells, one $5\frac{1}{2}$" wide with 100 cells, and the third $2\frac{1}{2}$" wide with 225 cells are used to guide and straighten the flow. Fig. (1) shows their optimum positions. To get a constant speed it is necessary to run the motor at its normal speed and to gear down the propeller. Several perforated plates are used in the channel as resistances. Throughout the whole circuit the channel is 5" wide and water of about 5" depth is used. The semicircular bend has an inner radius (a) of $2\frac{1}{2}$" and an outer radius of $7\frac{1}{2}$". Thus mean diameter (D) of the curve is 15" and width (H) is 5". Variation of velocity is

pitot?

detected by coupling one side of an inverted U-gauge to a pilot head at the upstream end, and the other end to a pressure box.

Coloured filaments were obtained by introducing aniline dye into the channel water from a reservoir shown ~~in Fig. (4~~). Fig. (1) shows the approximate position of this reservoir as used. The reservoir consists of a half inch diameter (of length $4\frac{3}{4}$") brass tube, with a cross piece at the centre. It is supported by two spring clips fixed to the bottom of a plate of length $5\frac{1}{2}$". A thin (bent into shape) tube $^3/32$" dia. communicates with the reservoir at two ends. Five holes 0.014" diameter are drilled on the upstream side of the transverse piece of the thin tube. The plate rests across the channel. The reservoir contains the dye - and the level of the dye is so adjusted that the dye just escapes through the five holes. The level of the dye in it is kept constant by feeding it through a capillary tubing from another vessel containing the dye, of the required concentration. The end of the capillary tube is kept submerged into the reservoir so as to prevent oscillation of surface otherwise to be caused by dripping. The plate is slotted and the cross piece is turned along the slot to fix the level at which the filament is to be introduced. The dilution of the dye had to be adjusted for different speeds, so that the filaments do not sink. This sets a limitation to the lowest speed at which photographs could be taken. At lowest speeds the dye had to be made so thin that photographs did not show the filaments. An idea of the speed is necessary to understand the difficulty. Thus for Reynold's number $\frac{Vm}{\nu} = 87$ where V is mean speed, m is the hydraulic mean depth $\frac{\text{Area}}{\text{Wetted perimeter}}$, the velocity is approximately equal to 0.098 inches per sec. At lower Reynold's Numbers, say for $\frac{Vm}{\nu} = 40$, and the speed of the order of 0.04"/sec., the dye was almost invisible and the slightest disturbance in the room upset the flow.

To provide a white background for photographic purposes the channel floor was lined with white cartridge paper which was covered with glass sheets of the required shape. An ordinary $\frac{1}{4}$ plate camera of focal length 10.5 cm. was used for photographing the filament lines with Ilford Panchromatic plates.

The average speed of the liquid flowing along the channel was obtained by taking the mean value of the speeds of water at the working section. The speed was measured by a Tilting Gauge devised and used previously by Dr. A. Thom (Ref. 2).

At certain speeds the water in the channel tended to oscillate - this was overcome by dividing the channel into compartments by means of perforated resistance plates. To prevent the surging of the water surface near the propeller a sheet of stiff cartridge paper was placed just touching the water surface there.

The effect of the propeller was noticeable before the extra length was added to the channel. The effect was tested by reversing the direction of the flow and feeding ink from the propeller end of the channel. This seems to have little or no effect after the channel has been lengthened.

The rise and the depression of a filament was measured by means of a point gauge by observing the filament at the straight portion and at seven sections throughout the bend. The gauge ~~is shown in Fig. (5) and~~ consists of a fine needle carried on an arm which slides over a graduated stand. As soon as the needle touches any filament it starts to waver.

Photographs are numbered A, B, C, D according to ~~depending on~~ the depths of the filament at the point of introduction, ~~The ones marked~~ A are ~~is~~ for a filament which is 4" above the floor of the channel initially ~~originally.~~ B. ~~is~~ for 3", C for 2", and D for 1".

Photographs for five different Reynolds number are attached (Plates 1, 2, 3, 4, 5). The Reynolds number for these vary from 467 to 103.

Table 1 gives the value of the lateral shift at 90° as obtained by measuring the photographs and of the vertical shifts as obtained by measuring the photographs and of the vertical shifts as obtained by the point gauge. The filaments are numbered from 1 to 5, the one near the convex side being No. 1. The lateral shift is marked (+) when the filament moves towards the concave side of the channel and the vertical side of the channel is marked (+) and fall (-).

At Reynolds number, approximately, 40 the filaments seemed to retain their original levels throughout the course. Photographs could not be obtained at such low Reynold's number since the average velocity required was of the order of 0.04" per sec.

DISCUSSION OF RESULTS.

At Reynold's number approximately equal to 40 the filaments show little sign of helical movement and the vertical movement is also negligible, showing that probably the internal circulation does not start until this Reynold's number, say N. So up to this we should expect the pressure gradient in the curves generally to correspond to that in the straight channel. This is probably the case as can be seen by comparing this figure with those of Grindley and Gibson, and of C. M. White for curved pipes. These are shown in Table (2) under the column headed N for different values of $\frac{d}{D}$ where d is the diameter of the pipe and D is the diameter of the coil. N is plotted on the base of $\frac{D}{d}$ logarithmically in Fig. (6). The graph is a straight line and the relation of (D/d) and N can be expressed as

$$N = C\left(\frac{D}{d}\right)^{\frac{1}{2}}$$

where C is approximately ~~4~~,12.

This also shows that the effect of curvature is to decrease the value of Reynold's number at which the circulation begins to develop, i.e., the point of the departure from the parabolic distribution of velocity. If this law holds then we should expect (D/d) equal to 25,120, where this graph cuts Reynold's Criterion to mark the point at which the flow in the curved pipe immediately departs from the viscous state to the turbulent state without passing through the stage during which the internal circulation begins to develop. In other words the effect of curvature is absent beyond (D/d)=24,120 and then the ordinary Reynold's Criterion will hold. Hence, Dean's Criterion $\frac{Fd}{\mu V} = f\left[\frac{e\,Vd}{\mu}\cdot\left(\frac{d}{D}\right)^{\frac{1}{2}}\right]$ would hold for curved pipes up to (D/d)=24,120.

The above conclusion may seem arbitrary, but the following consideration of Dean's paper on the stability of flow between coaxial cylinders lends weight to the argument. Dean considers the flow between the coaxial cylinders of radius a and A H and assume that $\frac{P}{e} = K\theta + f(r)$

where r = radius, P = pressure and $K, \not< 1$ and finds the exact solution for $U = W = 0$, $V = V_0$ and $p = P_0$. The constants, to satisfy boundaries of the cylinder $x = 0$ and $x = H$; are determined. Neglecting the terms of the relative order of H/a

$$V_0 = \frac{K}{2\nu a}(x^2 - xH) \qquad \textcircled{3}$$

This formula corresponds to Poiseuille's law. The effect of the curvature turn is only in the factor 1/a which is a constant for any one channel. Then he considers the stability for small disturbances of exactly type found by G. I. Taylor (Ref. 20) to answer for the instability of motion between two rotating cylinders.

The method is to consider small disturbance such that

$U = u$, $V = V_0 + v$, $W = w$ $P = P_0 + p$, where w, v, u are independent of θ Neglecting such terms as $\frac{1}{a+x}\frac{\partial u}{\partial x} - \frac{u}{(a+x)^2}$ in comparison with $\frac{\partial^2 u}{\partial x^2}$ he simplified the four hydrodynamical equations expressed in cylindrical coordinates. Then he finds out the non-zero solution of these equations subject to the boundary conditions $u = v = w = 0$ where $x = 0$, H . He gives the Criterion as

$$N = 36 \left(\frac{a}{H}\right)^{\frac{1}{2}} \qquad (4)$$

Below this value of N the disturbance is shown to be damped out. He suggests the form

$$N^2 \frac{d}{D} = \text{constant.}$$

as the possible form which will indicate the critical Reynold's number for the breakdown of the steady flow in a curved pipe. That this form does not hold true is seen when from the graph of $\mathrm{Log}_{10} R$ the critical Reynold's number for curved pipes is plotted against $\mathrm{Log}_{10} (D/d)$. C. M. White (Ref. 12) has shown that the critical speed for the curved pipes is given by

$$F/\varrho v^2 = 0.0045$$

and does not depend on either Reynold's or Dean's Criterion. It is clear from the methods employed by Dean as indicated above that this Criterion really marks the transition from steady viscous flow to steady double helical flow in the case of curved pipes, whereas in the case of pure two-dimensional flow since there could be no helical flow it must be the point of breakdown. It is thought that if disturbance of this type is considered on the flow

$$v = \frac{1}{4\mu}\left\{R^2 - r^2\right\}\frac{\partial p}{\partial x}$$

and above simplifying assumptioms made the Criterion should be got corresponding to

$$N = C\left(\frac{d}{D}\right)^{\frac{1}{2}}$$

C = 12 seems to be a round figure which such analysis may yield. The difficulty of the analysis of helical flow has been pointed out by Dean (Ref. 16).

The value N for this channel calculated according to this Criterion is approximately 25 calculated on two-dimensional basis; and as read from Fig. (6) it is 23. The value obtained from the present experiments if 40, but it must be remembered that the above Criterion applies when D/d or a/H is large.

Fig. (7) shows the paths of the filaments projected on the cross section for 90° turn for various Reynold's number. The paths are drawn approximately to show ~~up~~ the nature of the flow. The exact positions at the inlet end in the straight path and the final positions after 90° turn are accurate enough. These show the existence of a double circulation. Figs. (8) and (9) show the nature of the circulation existing at 90° as drawn from the approximate slopes of the filaments at this section. The sense of the filaments is shown in full and the circulation in dotted lines.

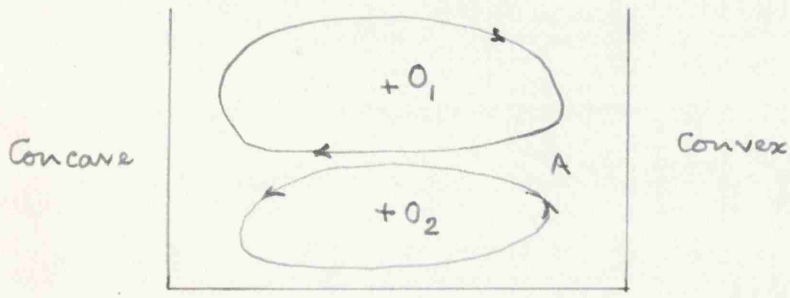

FIG 10

Fig. (10) shows the general position of this circulation. If such a circulation exists then the filaments near the concave end will tend to be lifted up and go towards the convex side; or to be depressed and go further towards the convex side, depending on the position occupied by the filaments with respect to the circulation. Near the convex side the reverse effects are to be noticed. The maximum lateral shift will occur in the region A and there will be no movement of the filaments in the regions O_1 and O_2. As these movements are all shown in the measurements the circulation diagrams 8 and 9 probably represent the actual state of flow.

Comparing the diagrams in Fig. (7) and 8 and 9, it is to be noticed that the two circulations seem to divide the cross section approximately into trapezoidal parts instead of rectangles.

A probable explanation of this is to be seen by comparing Fig. (3) for circular tubes. The line of separation of these two circulations is the line joining the points furthest away and nearest, i.e. where the centrifugal force is greatest to the origin of reference where the centrifugal force is the least. The origin of reference lies on the plain of symmetry, which is also the plane of maximum ~~philosophy~~ velocity. In the case of a channel taking the plane of reference as the plane in which the filament of maximum velocity lies - this plane is somewhat below the free surface of water - Th~~is~~ point furthest away from the centre of the curve of the channel is the corner at the concave end and the nearest point is on the convex side. The centrifugal force is the greatest at the concave edge and the least near the convex surface. Thus the separation of the circulations takes place in a line inclined to horizontal.

Comparing Figs. (8) and (9) it will be noticed that the bottom circulation is more important than the top circulation as the speed diminishes. This is also seen from a study of diagrams in Fig. (7). This demonstrates the fact that the transverse inclination of the free level is the main driving force in causing the top circulation. Otherwise we should get a comparatively small region of top circulation at all speeds like that in Fig. (9).

At high speed the top circulation is more strong and the water as it were runs down the hill. At low speeds the transverse inclination of the free surface is small and so the bottom circulation is more important.

Another conclusion to be drawn from comparison of the diagram of parts of filaments as shown in Fig. (7) is that the circulation gets weaker as the speed diminishes. The rise and the depression of the filaments form a surer guide to show this fact than lateral shift - because even with pure two-dimensional flow there is certain amount of lateral shift of the filament lines from the original positions in the straight part. That this is the case will be shown in the solution given in Part II of this paper for irrotational motion. At any rate a comparison of plates (5) which is for R = 103 with others will show that the top circulation is negligibly smaller as compared to the bottom circulation which is also weak as compared to that for other values of R.

Plates (5) d shows the diffusion of the dye in the viscous layer near the floor of the channel.

The existence of the slow-rising water from the bottom between the water of comparatively high velocity and the convex bank is to be noticed from Figs. (8) and (9); that this exists at all speeds between Reynold's Number 40 and the critical can be observed from a study of the Plates 1-5. Even in Plate (1) for R = 467 the filaments leave a clear space near the convex side before they start on their downward journey. This is more marked at lower speeds. Beyond the critical still there exists this cushion of water near the convex side. Fig. (11) gives rough sketch of the cross profile of the water surface. The hump near the convex edge shows the existence of this slow-moving water; so it seems that James Thomson's theory of Meanderings of Rivers in Alluvial Plains is true. (Ref. 1).

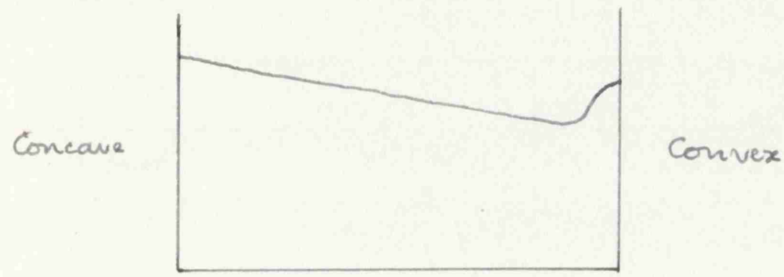

FIG 11

There is a further effect. The filament of maximum velocity will shift its position due to this top circulation. The filament of maximum velocity will be depressed at all times between the convex bank and the central line and raised at all points between the concave side and the central line due to the existence of this top circulation.

From Plate (5A, R=103) it is to be noticed that the flow pattern is almost symmetrical. This shows an approach to two-dimensional states. A comparison of this plate with that of Fig. (13) will show the resemblance of these two.

The Critical flow for the channel as obtained by the determination of the speed at which a single filament of dye starts waving with growing amptitude is found to occur at

$R = \frac{Vm}{\nu} = 757$ for the straight portion, and at $R = \frac{Vm}{\nu} = 647$ for the curved channel. This is quite contrary to that found by C. M. White (Ref. 12) and G. I. Taylor (Ref. 11) for curved pipes. The effect of curvature seems to be to raise the Critical speed for turbulence in curved pipes as seen from the column headed R_c in Table 11. C. M. White's experimental Criterion for turbulence in curved pipe is

$$F/\rho v^2 \doteq 0 \cdot 0045$$

irrespective of curvature. The Critical flow should occur at R = 4,000 instead of observed 647 if the law for curved pipe could be applied to the curved channel. Here again we should bear in mind that the case for channel is intermediate between pure two-dimensional flow and the three-dimensional flow. Instability sets in at R = 25 for pure two-dimensional flow as indicated before. The ~~Fig.~~ figure 647 seems to be a reasonable figure seeing that the channel is intermediate between these two extreme cases. There is the further point that at high Reynold's Number the top circulation is by far out of balance in comparison with the bottom circulation and the probable net effect is to lower the Critical velocity below that for a straight channel.

<u>Conclusions</u>.

From the above discussions the fluid flow in a channel bend may be divided into four stages, viz.:-

(1) Stage during which the pressure lost is the same as that for a straight channel and the flow is probably of two-dimensional nature.

(2) Stage during which the bottom circulation is more pronounced than the top circulation.

(3) Stage with dominating top circulation.

(4) Stage beyond the Critical speed during which it is believed that the top circulation still exists because of the inclination of the free surface; contrary to that for pipes where no internal circulation exists beyond the Critical speed.

From the photographs it is evident that a Yaw Head is necessary to investigate the velocity distribution in the curved path of the channel. Since the channel is so small a three-dimensional Yaw Head will upset the flow.

The use of this bend at the exit end of the straight portion of the channel does not seem to affect the flow pattern beyond a distance of the order of 2H to 3H. This varies a little with Reynold's number. The stream lines start converging then. The vertical movement is not noticeable just at the entrance to the bend. The circulation seems to develop at above 10 - to 15 degrees away downstream from the entrance to the bend.

The straight length up to which the use of the bend as entrance space will affect the velocity distribution could not be determined. The filaments lost their identity after travelling about 10" from the exit of the channel. Up till then the filaments had not regained their original configurations. This certainly does not commend the use of this bend as an entrance to such a channel.

PART II.

This part deals with the arithmetical method of solving the stream function field for the semicircular bend in question. The solution given here is for irrotational motion of perfect fluid.

The equations of steady motion for perfect fluid in two dimensions are:-

$$u \frac{\partial u}{\partial x} + v \frac{\partial u}{\partial y} = -\frac{1}{\rho} \frac{\partial p}{\partial x} \quad \cdots \quad (7)$$

$$u \frac{\partial v}{\partial x} + v \frac{\partial v}{\partial y} = -\frac{1}{\rho} \frac{\partial p}{\partial y} \quad \cdots \quad (8)$$

and the equation of continuity is:-

$$\frac{\partial u}{\partial x} + \frac{\partial v}{\partial y} = 0 \quad \cdots \quad (9)$$

Introducing the function ψ, the stream function, for irrotational motion such that

$$\left.\begin{aligned} u &= -\frac{\partial \psi}{\partial y} \\ v &= \frac{\partial \psi}{\partial x} \end{aligned}\right\} \quad \cdots \quad (10)$$

the equations of motion reduce to:-

$$\nabla^2 \psi \equiv \frac{\partial^2 \psi}{\partial x^2} + \frac{\partial^2 \psi}{\partial y^2} = 0 \quad \cdots \quad (11)$$

The solution involves satisfying the boundary conditions. The method of solution adopted is due to Dr. A. Thom. (Ref. 22). The method consists in dividing the field of flow into squares, assigning the proper boundary values and assuming corner values to these squares. Then the centre values of these squares are calculated from the formula

$$\psi_0 = \psi_M \qquad (12)$$

where ψ_0 is the value of the stream function at the centre $\psi_M = (\psi_1 + \psi_2 + \psi_3 + \psi_4) \div 4$, ie the mean of the corner values of the stream functions.

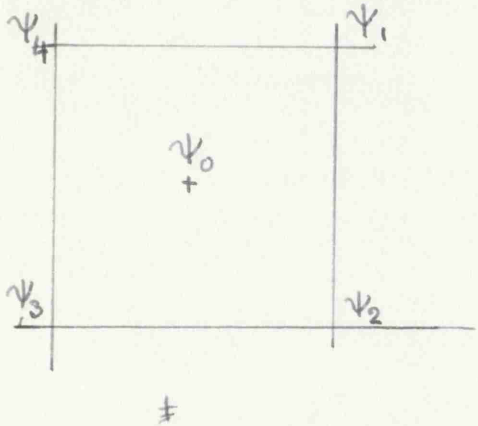

These centre values which also lie at the corners of squares are treated in the same way to find a better value for the original corners of the squares to be used in turn again. The convergence of this method has been demonstrated by Dr. A. Thom by applying this method for several cases of fluid flow and torsion problems.

The bend is accurately drawn on a square paper. The boundary values are assumed to be $\psi = 0$ for the outer wall and $\psi = 100$ for the inner wall. The values on the axis of symmetry of the bend are calculated from the Rankine Vortex formula.

The stream lines are roughly sketched joining the points on the axis of symmetry and a few equally spaced points far out in the straight portion. The corner values are then read off. This gives a start for applying equation (12) to improve the field further. The process of successive approximation is repeated until the stream function values at the corner of the squares do not move appreciably. The difficulty presented in the present case is due to the existence of carved boundaries. The corner values of squares falling near the boundaries are improved by extrapolation after two or three rounds. The field is then divided into smaller squares and the procedure is repeated. This eventually gives a fairly good solution of the field. If the process is repeated far enough a solution of great accuracy can be obtained. Fig. (12) shows the portion of the field as divided into squares with stream ~~extreme~~ function values. Fig. (13) shows the stream lines as drawn for this field. The equipotential lines are also shown. These however have been drawn by mechanical construction and the writer does not profess to give them with the same accuracy as the stream lines.

It is to be noted that the ψ values on the axis of symmetry are quite different from those of the Rankine Vortex.

The bend does not seem to affect the field on the straight portion to a great length. The stream function values are not affected more than 0.1 per cent at a distance of about 2 H where H is the distance between the walls.

A glance at the diagram shows that the stream lines tend to converge as it enters the bend and diverges and finally is straightened ~~driven~~ out at the exit end.

A comparison of Fig. (13) and Plate (5a) shows that at $R = 103$ for the semicircular channel the flow patterns closely resemble each other. At $R = 40$ for the channel the flow pattern was almost identical.

Hele Shaw (Ref. 23) experiments have shown that the flow pattern for infinitely viscous flow and that calculated for perfect fluid are identical in form. These have been shown to be mathematically correct by Sir George Stokes (Ref. 24). If this is so then the field shown in Fig. (13) is the same as that for $\nabla^4\psi = 0$ only the values of ψ for the stream lines are different. These values can be obtained by the knowledge of the ψ values at the straight portion and can be calculated from the equation of viscous flow between parallel walls. At any rate Plate (5a) certainly shows the stage at which internal circulation is dying out.

In conclusion the writer wishes to thank Professor J. D. Cormack for granting him facilities for work in connection with this paper. To Dr. A. Thom the writer is indebted for criticisms and suggestions during the experiments and the writing up of the paper. The writer is also indebted to the Trustees of the Department of Scientific and Industrial Research for the grant which enabled him to carry out this and other works during the year 1931-1932.

Tabke I.

Filament No	Original Distance from Convex Side	Horizontal Shift in inches				Vertical Shift in inches				R
~~66~~	"	A	B	C	D	A	B	C	D	
I	0,72	0,80	I,75	I,40	I,22	-I,I0	-0,90	-0,50	0,I0	
2	I,60	0,53	I,28	0,87	0,80	-0,60	-0,20	-0,I0	-0,I0	
3	2,50	-0,95	0,8I	0,38	0,27	-0,20	o0,70	0,60	-0,20	467
4	3,40	-2,I0	0,09	-0,32	-0,49	-0,70	I,20	I,00	-0,80	
5	4,30	-3,45	-0,38	-0,84	-I,I4	-0,70	0,90	2,00	-I,00	
I	0,70	I,70	I,90	2,20	I,73	-I,6I	-0,9I	-0,2I	0,I9	
2	I,60	0,76	I,64	I,67	I,40	0,I6	0,04	0,I2	-0,00	
3	2,50	-0,60	I,30	I,22	0,63	0,43	0,95	0,08	-0,20	390
4	3,40	-2,24	0,I4	0,62	-0,36	-I,I5	I,20	0,80	-0,80	
5	4,30	-3,09		-0,0I	-I,50	-0,I6	0,7I	0,9I	-0,64	
I	0,70	I,74	I,74	2,I0	I,82	-I,55	-I,I0	-0,70	0,I0	
2	I,60	0,64	I,50	I,76	I,50	-I,30	-0,60	-0,60	-0,I5	
3	2,50	-0,I2	I,02	I,26	I,I0	-I,I0	0,20	0	-0,60	376
4	3,40	-I,9I	0,09	0,80	0,I4	0,08	I,50	0,28	0,7I	
5	4,30	-3,2I	-I,30	0,I8	-I,32	-0,20	2,I0	2,00	-0,35	
I	0,70	2,I3	2,24	0,74	0,40	-I,05	-0,90	-0,47	-0,20	
2	I,60	0,90	I,77	I,40	I,00	-0,24	-0,36	-0,I6	-0,20	
3	2,50	-0,I6	I,27	I,I6	0,64	0,5I	0,I6	-0,04	-0,55	324
4	3,40	-I,50	0,I4	0,60	-0,I6	0,24	-0,47	-0,98	0,I2	
5	4,30	-2,96	-2,39	0,02	-I,24	0,43	I,I0	I,42	-0,75	
I	0,70	0,I7	0,5I	0,75	0,42	-0,63	-0,67	-0,I8	2,40	
2	I,60	-0,47	0,22	0,67	-0,80	-0,08	-0,67	-0,35	-I,78	
3	2,50	-0,97	-0,25	0,27	-I,2I	0,I6	-0,59	-0,67	-I,03	I03
4	3,40	-I,28	-0,85	0,0I	-2,22	0,32	0,83	0,32	-0,I3	
5	4,30	-I,48	-I,00	-0,I7	-3,86	0,04	-0,39	-I,50	3,60	

Note:- A 4'' above floor
B 3'' ,, ,,
C 2'' ,, ,,
D I'' ,, ,,

Table II

D/d	Critical N	Critical R_c	Remarks
15,15	50	9000 (7590)	White
18,70	-	7100 (5830)	Taylor
31,90		6350 (5010)	,,
50,00	80	6000 (6020)	White
112,00	130		Grindley and Gibson
2050,	550	2250 (2270)	White
3,00	40	647	Present Experiments for channel.

REFERENCES.

(1) On the Origins of Windings of Rivers in Alluvial Plains with remarks on the flow round bends in pipes - by James Thomson - Proc. Royal Soc., London, Vol. 25 (1876), pp. 5-8; also Vol. 26 (1877), pp. 356-57.

(2) R. M. No. 1389 - The Pressure on the Front Generator of a Cylinder - by A. Thom - (Dec. 1930). H. M. Stationery Office.

(3) Hydraulics and its Applications - by A. H. Gibson, Fourth Edition, 1930, pp. 327-28. (Constable).

(4) Flow of water in curved pipes - by J. Eustice - Proc. Royal Soc. Lond., A.84, pp. 107-118 (1910).

(5) Experiments on Streamline Motion in Curved Pipes - J. Eustice - Proc. Roy. Soc. Lond., A. 85, pp. 119-131 (1911).

(6) Flow of water in Pipe Bends - by J. Eustice - Water and Water Engineering. July-Nov. (1924).

(7) Flow of water in curved passages - by J. Eustice - Engineering, Vol. 120, pp. 604-605 (1925).

(8) Flow in Curved Channels - by A. Hinderks. Z. Vor. Deut. Ing., Vol. 71, pp. 1779-1783 (1927), also see Bulletin Nat. Research Council, No. 84 (p. 485), Washington (1931).

(9) Note on the Motion of Fluid in Curved Pipe - by W. R. Dean. Phil. Mag. S. 7, Vol. 4, pp. 208-223 (1927).

(10) The Stream Line Motion in a Curved Pipe - Second Paper - by W. R. Dean. Phil. Mag. S. 7, Vol. 5, pp. 673-695 (1928).

(11) The Criterion of Turbulence in Curved Pipes - by G. I. Taylor - Proc. Royal Soc. Lond. See A. 124, pp. 243-249 (1929).

(12) Stream Line Flow through Curved Pipes - by C. M. White; Proc. Roy. Soc. Lond., Sec. A. 123, pp. 645-663 (1929).

(13) Modern Aerodynamical Research in Germany - by J. W. Maccoll; Journal of the Royal Aeronautical Society, No. 236, Vol. 34, pp. 649-689, August (1930).

(14) Bulletin of the National Research Council, No. 84. Report of the Committee on Hydrodynamics, pp. 481-92, (1931) Washington.

(15) Vortrage aus dem Gebiete der Aerodynamik und verwandter Gebiete Aachen, 1929, pp. 10-18, Springer, Berlin.

(16) Fluid Motion in a Curved Channel - by W. R. Dean - Proc. Royal Soc. Lond., Sec. A, 121, pp. 402-420 (1928).

(17) Meanderings of Alluvial Rivers governed by a fixed law - by P. Claxton. Engineering News Record, Vol. 99, No. 7, p. 268 (1927).

(18) Report on the physics and hydraulics of the Mississipi River by A. A. Humphreys and H. L. Abbot (1861), Philadelphia.

(19) On the Frictional Resistances to the flow of air through a pipe, by J. H. Grindley and A. H. Gibson - Proc. Royal Soc. Lond., Sec. A, Vol. 80, pp. 114-139 (1908).

(20) The motion of Viscous Fluid within Two Rotating Cylinders - by G. I. Taylor, - Philosophical Transaction of the Royal Soc., Vol. 223, p. 289.

(21) The Depression of the Filament of Maximum Velocity in a Stream flowing through an open Channel - by A. H. Gibson - Proc. Royal Soc. Lond., Sec. A, Vol. 82, pp. 149-159 (1909).

(22) R. M. 1194. An Investigation of Fluid Flow in two-dimensions by A. Thom (Nov. 1920). H.M.S.Office; also, The Solution of Torsion Problems for Circular Shaft of Varying Radius - by A. Thom and J. Orr - Proc. Royal Soc. Lond., Sec. A, Vol. 131, pp. 30-37 (1931).

(23) Trans. Institute Naval Architect., p. 27 (1896).

(24) Mechanical Properties of Fluids, pp. 155-156 - Blackie (1925); also British Assoc. Reports, pp. 143-144 (1898).

List of Diagrams.

List of Plates.

List of Tables.

163

AIR MINISTRY
For Official Use

R. & M. No. 1520

AERONAUTICAL RESEARCH COMMITTEE
REPORTS AND MEMORANDA No. 1520
(T.3319)

Air Torque on a Cylinder Rotating in an Air Stream

By A. THOM
D.Sc., Ph.D. AND
S. R. SENGUPTA

Communicated by Prof. J. D. CORMACK

OCTOBER 1932

LONDON
PRINTED AND PUBLISHED BY HIS MAJESTY'S STATIONERY OFFICE
To be purchased directly from H.M. STATIONERY OFFICE at the following addresses
Adastral House, Kingsway, London, W.C.2; 120, George Street, Edinburgh 2
York Street, Manchester 1; 1, St. Andrew's Crescent, Cardiff
15, Donegall Square West, Belfast
or through any Bookseller

1933
Price 6*d*. Net

23-9999